Spectral properties of the dimerized and frustrated $S=1/2$ chain

Kai P. Schmidt, Christian Knetter, and Götz S. Uhrig
Institut für Theoretische Physik, Universität zu Köln, Zülpicher Strasse 77, D-50937 Köln, Germany
(Received 25 July 2003; published 22 March 2004)

Spectral densities are calculated for the dimerized and frustrated $S=1/2$ chain using the method of continuous unitary transformations. The transformation to an effective triplon model is realized in a perturbative fashion up to high orders about the limit of isolated dimers. An efficient description in terms of triplons (elementary triplets) is possible: a detailed analysis of the spectral densities is provided for strong and intermediate dimerization including the influence of frustration. Precise predictions are made for inelastic neutron scattering experiments probing the $S=1$ sector and for optical experiments (Raman scattering, infrared absorption) probing the $S=0$ sector. Bound states and resonances influence the important continua strongly. The comparison with the field theoretic results reveals that the sine-Gordon model describes the low-energy features for strong to intermediate dimerization only at critical frustration.

DOI: 10.1103/PhysRevB.69.104417 PACS number(s): 75.40.Gb, 75.50.Ee, 75.10.Jm

I. INTRODUCTION

One-dimensional quantum antiferromagnets display very interesting and fascinating physical properties. The generic system to be studied in this context is the dimerized and frustrated Heisenberg chain which comprises many physical phenomena of interest. There are gapless and gapped phases,[1] fractional excitations,[2,3] and confinement.[1]

The quantitative calculation of spectral densities is a very important issue in the field of strongly correlated electron systems. The interplay between kinetics, interaction, and matrix elements leads to characteristic structures in the spectra. In recent years there has been significant progress in calculating spectral densities in the field of quasi-one-dimensional quantum spin systems, e.g., the uniform Heisenberg chain,[4] spin ladders systems,[5,6] and strongly dimerized spin chains.[7,8]

Besides the fascinating theoretical aspects, the determination of spectral densities is of direct importance for experimental measurements. The theoretically predicted spectra are relevant for inelastic neutron scattering experiments and optical experiments like Raman spectroscopy and infrared absorption. There is a large number of quasi-one-dimensional compounds which can be successfully described by the dimerized and frustrated Heisenberg model, e.g., spin-Peierls compounds such as $CuGeO_3$ (Refs. 9–12) and α'-NaV_2O_5,[13] $(VO)_2P_2O_7$ (Ref. 14) or organic compounds such as $Cu_2(C_5H_{12}N_2)_2Cl_4$ (Ref. 15) and $[Cu(NO_3)_2 \cdot 2.5D_2O]$.[16,17] The limit of vanishing dimerization is realized in the cuprate chain compounds such as $KCuF_3$,[18] Sr_2CuO_3,[19] and $SrCuO_2$.[20]

We will describe the dimerized and frustrated spin chain in terms of elementary triplets (triplons) (Ref. 21) which carry total spin one. The commonly accepted elementary excitations for the *undimerized* system are fractional excitations, so-called spinons, carrying $S=1/2$.[2,3] Recently we have shown that a description in terms of triplons is also possible for the isotropic Heisenberg chain.[22] So there is no necessity to use fractional excitations in one-dimensional systems. Remarkably, even more spectral weight is captured by the states of two triplons than with two spinons.[22] This result was recently confirmed by Hamer *et al.*[8]

In this work, we take a closer look at the generic features of the spectral properties at finite dimerization. In this regime a description in terms of triplons is surely correct due to the confinement of the spinons.[1] We will learn more about the triplon picture and try to connect the triplon-based findings at finite dimerization with results obtained at zero dimerization using the spinon picture.

The paper is organized as follows. Section II gives an introduction to the model. Section III presents the method we use and introduces the basic quantities under consideration. In Sec. IV results for the dynamical structure factor are shown. We present results for the one-triplon contribution, the two-triplon contribution and compare with field theoretical results. Section V shows spectral densities with total spin zero. We give results for the two-triplon contribution for nearest-neighbor (NN) and next-nearest-neighbor (NNN) coupling. We also provide results for Raman spectroscopy and optical absorption. Section VI summarizes this paper and Sec. VII comprises the conclusions.

II. MODEL

The Hamiltonian for the dimerized and frustrated $S=1/2$ spin chain reads

$$H=J_0\sum_i \{[1+\delta(-1)^i]\mathbf{S}_i\mathbf{S}_{i+1}+\alpha_0\mathbf{S}_i\mathbf{S}_{i+2}\}, \qquad (1)$$

where δ parameterizes the dimerization and α_0 the relative frustration between NNN spins. In order to apply a perturbative treatment we transform Eq. (1) into

$$H/J=\sum_i [\mathbf{S}_{2i}\mathbf{S}_{2i+1}+\lambda\mathbf{S}_{2i}\mathbf{S}_{2i-1}+\lambda\alpha\mathbf{S}_i\mathbf{S}_{i+2}], \qquad (2)$$

where $J=J_0(1+\delta)$, $\lambda=(1-\delta)/(1+\delta)$, and $\alpha=\alpha_0/(1-\delta)$.

The dimerized and frustrated spin chain exhibits very interesting intrinsic physics. The phase diagram of the model is shown in Fig. 1. At $\delta=0$ there are two regimes.

 ©2004 The American Physical Society

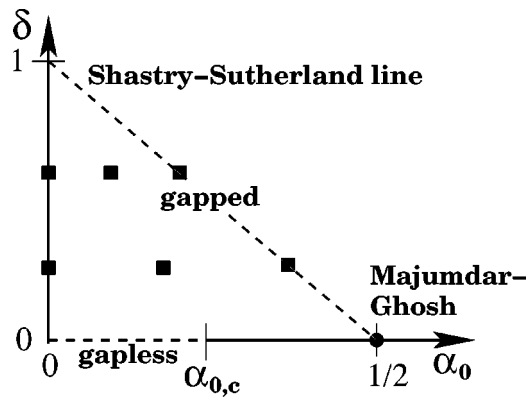

FIG. 1. Phase diagram of the dimerized and frustrated Heisenberg chain depending on frustration α_0 and dimerization δ. The system is always in a gapped regime except in the interval $\alpha_0 \in [0,\alpha_{0,c}]$ at zero dimerization. The dashed line marks the Shastry-Sutherland line where the ground-state is known exactly. Solid squares correspond to the parameters $(1-\delta)/(1+\delta)=\lambda \in \{0.3;0.6\}$ and $\alpha_0/(1-\delta)=\alpha \in \{0.0;0.25;0.5\}$ used in this work.

(i) For $\alpha_0 < \alpha_{0,c}$ the ground state is in the same universality class as the uniform Heisenberg chain. The excitations are massless and the standard description is in terms of unconfined spinons carrying total spin $S=1/2$.[2,3] In a recent work we have shown that also a description in terms of triplons is appropriate for the isotropic Heisenberg chain.[22]

(ii) At $\alpha_0=\alpha_{0,c}$ there is a transition into a spontaneously dimerized phase.[12,23–25] The ground state is two-fold degenerate and the excitations are massive spinons for $\alpha_0 > \alpha_{0,c}$. At the Majumdar-Ghosh point ($\alpha_0=0.5$) the ground-state is known exactly.[26–28] The validity of a triplon description in this gapped phase is an open issue. On the other hand, Haldane[1] has shown that for any finite dimerization δ the spinons become confined and a description in terms of triplons carrying total spin $S=1$ is appropriate. The spectrum is always gapped[1,29,30] and the excitations can be viewed as bound states of two spinons.[31–34] The interaction between the spinons is not exhausted by the confinement and there remains a triplon-triplon interaction which can lead to two-triplon bound states with total spin $S=0$ and $S=1$ lying below the multitriplon continuum.[29,33,35–41]

Spectral properties are particularly difficult to address. So far, results can be obtained either by numerical approaches such as exact diagonalization or quantum Monte Carlo or by studies of effective continuum models. In particular, the case of finite frustration and the $S=0$ sector relevant for optical experiments has not yet been investigated thoroughly.

In the following we expand about the limit of isolated dimers on the strong bonds, i.e., $\lambda=0$. We present results for the two-triplon contribution to the spectral density for strong ($\lambda=0.3$) and intermediate ($\lambda=0.6$) dimerization and for three representative values of the frustration ($\alpha=0$, $\alpha=0.25$, $\alpha=0.5$). These parameters are marked in Fig. 1 as filled squares.

III. METHOD

A continuous unitary transformation[42] is used to map the Hamiltonian H to an effective Hamiltonian H_{eff} which conserves the number of triplons on the strong bonds, i.e., $[H_0,H_{\text{eff}}]=0$ where $H_0 := H|_{\lambda=0}$.[43,46] The ground state of H_{eff} is the triplon vacuum. Using an infinitesimal anti-Hermitian generator η we have

$$\frac{dH}{dl}=[\eta(l),H(l)], \tag{3}$$

where $H(0)=H$, $H(\infty)=H_{\text{eff}}$ and $l \geqslant 0$ is an auxiliary variable. The optimized choice for η reads

$$\eta_{i,j}(l)=\text{sgn}([H_0]_{i,i}-[H_0]_{j,j})H_{i,j}(l), \tag{4}$$

where the matrix elements $\eta_{i,j}$ and $H_{i,j}$ are given in an eigen basis of H_0 counting the number of triplons on the strong bonds. The choice (4) retains only triplon conserving processes and it eliminates all parts of H changing the number of triplons.[43] It must be stressed that the approach represents a renormalization in the sense that matrix elements between states with very different energies are transformed strongest in the early stages of the transformation. The matrix elements between energetically similar states are transformed only at a later stage of the transformation.

In order to determine spectral weights I_n and spectral densities the observable R is mapped to an effective observable R_{eff} by the same unitary transformation[46] (3) as the Hamiltonian.

The continuous unitary transformation cannot be carried out without truncation. We use a perturbative method in λ. The effective Hamiltonian H_{eff} is calculated up to order 10 and the effective observable R_{eff} is calculated up to order 7 in the two-triplon sector. The plain series of the important quantities will be made available on our home pages.[44] Details of the calculation will not be presented here. They are given exemplarily for the spin ladder in Ref. 45.

The following extrapolation technique is employed, which we have introduced recently for spin-ladder systems.[47,48] After fixing α to the desired value the plain series in λ is converted into a series in $1-\Delta$ invoking the one-triplon gap Δ. The one-triplon gap is the natural internal energy scale of the problem. Since in this work we are interested only in strong and intermediate dimerization, no further extrapolation techniques such as standard Padé extrapolants are used. There is no uncertainty in the obtained spectral densities for strong dimerization $\lambda=0.3$. The uncertainty is about 2% of J for the worst case at intermediate dimerization ($\lambda=0.6$). In order to investigate the cases of weak or vanishing dimerization it would be important to use further extrapolation tools and to treat processes with longer or infinite range explicitly.

At $T=0$, spectral densities can be calculated from the retarded Green function

$$I(\omega)=-\frac{1}{\pi}\text{Im}\langle 0|R^{\dagger}\frac{1}{\omega-(H-E_0)+i0+}R|0\rangle. \tag{5}$$

Due to the conservation of triplons after the unitary transformation the spectral density can be split into additive parts $I_n(\omega)$, the n-triplon contribution to the spectral density,

$$I(\omega)=\sum_n I_n(\omega), \tag{6a}$$

$$I_n(\omega)=\frac{-\mathrm{Im}}{\pi}\langle 0|R^{\dagger}_{\mathrm{eff,n}}\frac{1}{\omega-H^{(n)}_{\mathrm{eff}}+i0+}R_{\mathrm{eff,n}}|0\rangle, \tag{6b}$$

where $H^{(n)}_{\mathrm{eff}}=\Sigma^{n}_{i=1}H_{\mathrm{eff,i}}$. For the precise definitions of the operators $H_{\mathrm{eff,i}}$ and $R_{\mathrm{eff,i}}$ the reader is referred to Ref. 45. The total intensity can be calculated using Dirac's identity for Eq. (5):

$$I_{\mathrm{tot}}=\int_{0+}^{\infty}d\omega I(\omega)=\langle 0|R^{\dagger}_{\mathrm{eff}}R_{\mathrm{eff}}|0\rangle. \tag{7}$$

The total intensity I_{tot} is a sum over the spectral weight of all triplon sectors, $I_{\mathrm{tot}}=\Sigma_{n>0}I_n$. The spectral weight I_n in the n-triplon sector is calculated by

$$I_n=\langle 0|R^{\dagger}_{n,\mathrm{eff}}R_{n,\mathrm{eff}}|0\rangle, \tag{8}$$

where $R_{n,\mathrm{eff}}$ denotes all n-triplon excitation processes of the observable R. Using the sum rule $I_{\mathrm{tot}}=\langle 0|R^2|0\rangle-\langle 0|R|0\rangle^2$ we can check the reliability of the perturbative results. For later use we define the relative spectral weights $I_{n,\mathrm{rel}}=I_n/I_{\mathrm{tot}}$ with $\Sigma_{n>0}I_n/I_{\mathrm{tot}}=1$.

IV. $S=1$ EXCITATIONS

This part of the paper contains results for the dynamical structure factor of the dimerized and frustrated spin chain. At $\lambda=0$ the system consists of isolated dimers and therefore the total spectral weight is in the one-triplon channel I_1. Turning on λ will reduce the spectral weight in the one-triplon channel and the spectral weight will also be distributed over the multi-triplon channels. In the unfrustrated chain the spectral weight is shifted almost totally from the one-triplon channel to the two-triplon channel on passing from strong to zero dimerization.[22] In an analogous procedure we have analyzed the spectral weight distribution on the disorder line at $\alpha=0.5$. We find indications that again the two-triplon contribution is the dominant one, even for vanishing dimerization. But due to the complexity of the frustrated system no unambiguous extrapolations are possible.[49] Thus we do not have a final answer for the massive frustrated phase.

In the following we will show results for the one-triplon and the two-triplon contribution to the spectral density. The one-triplon contribution contains most of the spectral weight at strong and intermediate dimerization. In the limit of small dimerization it is highly reduced and becomes unimportant for zero dimerization. We expect that the two-triplon contribution is the only relevant contribution in the limit of zero dimerization.[22]

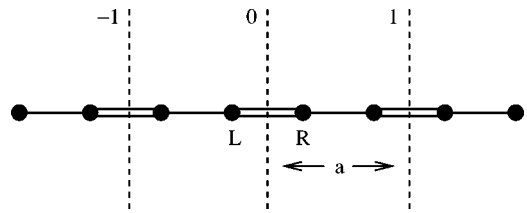

FIG. 2. Sketch of the local observable for $S=1$ excitations. Double lines denote strong bonds and single lines weak bonds. The observable couples to the left (L) and to the right (R) spin of a strong bond.

A discussion of the one-triplon contribution to the dynamic susceptibility of a dimerized chain without frustration can be found in a work by Müller and Mikeska.[50] Recently Zheng *et al.* published results for the one- and two-triplon contribution of a strongly dimerized spin chain without frustration.[7] Our results at zero frustration agree with the findings of Zheng *et al.*

Here we want to extract the generic features of the two-triplon contribution for various dimerization and frustration in order to gain insight in the evolution of this contribution in the limit of vanishing dimerization. Therefore it is interesting to compare our results with results for the dynamical structure factor at zero dimerization.

At $\alpha=0$ an exact calculation of the two-spinon contribution to the dynamical structure factor using Bethe-ansatz is possible.[4] The two-spinon contribution exhausts 72.89% of the total spectral weight and it displays a singular divergent behavior at the lower edge of the two-spinon continuum. At finite frustration only numerical results using exact diagonalization at finite temperatures including frustration are available.[51] In addition, there are also results using Abelian bosonization extracting the universal features of the dynamical structure factor at low energies for small dimerization.[34] In the following we will identify the major features of these studies in our triplon description at finite dimerization.

A. One-triplon contribution

The local physical observable $R^{S=1}$ for total $S=1$ excitations reads

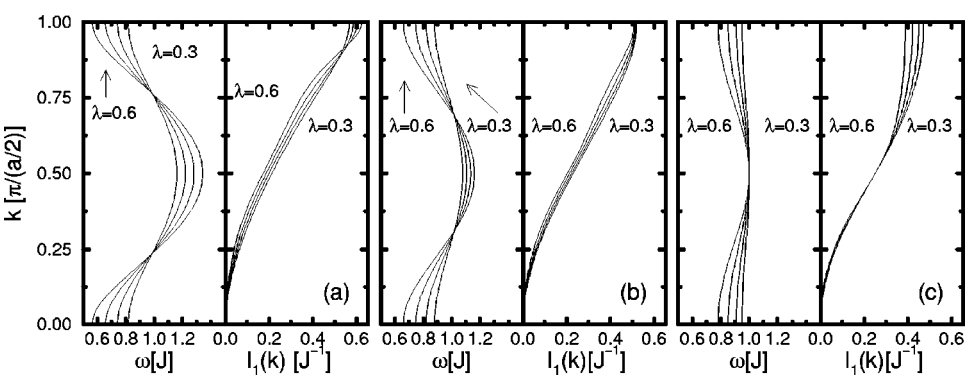

FIG. 3. One-triplon dispersion $\omega(k)$ (left panels) and one-triplon spectral weight $I_1(k)$ (right panels) for $\lambda=\{0.3;0.4;0.5;0.6\}$. In (a) $\alpha=0.0$, in (b) $\alpha=0.25$, and in (c) $\alpha=0.5$.

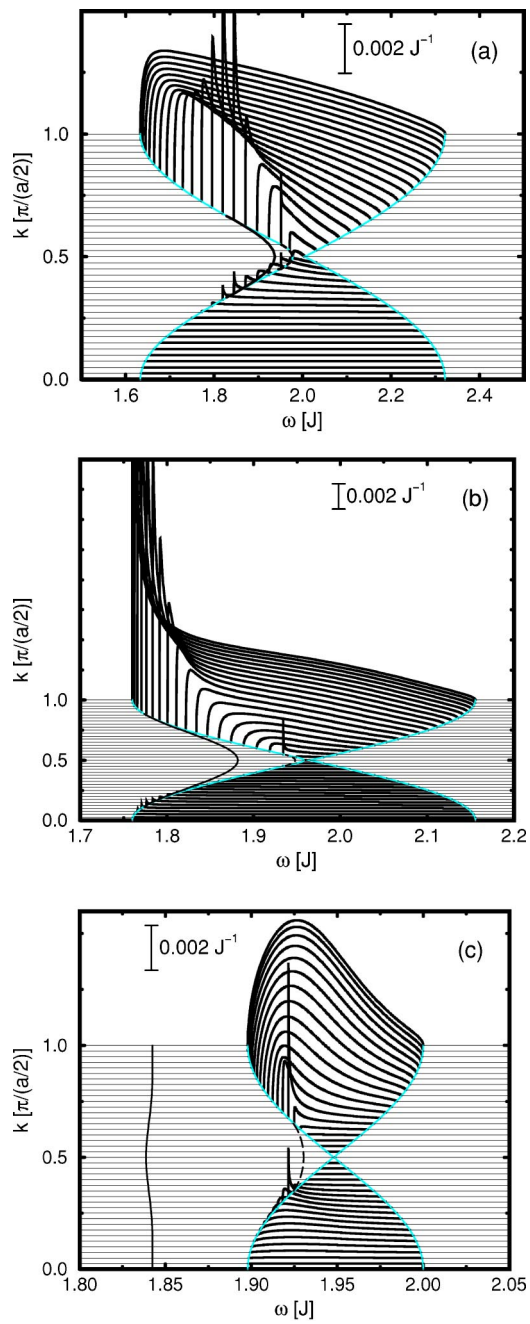

FIG. 4. Two-triplon spectral density $I_2(k,\omega)$ for $R^{S=1}$ with $\lambda=0.3$ and $\alpha=0.0$ (a), $\alpha=0.25$ (b), and $\alpha=0.5$ (c). Gray lines denote the lower and upper bound of the continuum. Black lines indicate dispersion of two-triplon bound states.

$$R_{\mathrm{loc}}^{S=1}=S_i^{\mathrm{z}}, \tag{9}$$

where i denotes a site of the chain. In the following we will denote the left and the right site on a strong bond by L and R, cf. Fig. 2. We decompose the action of the full observable $R^{S=1}|_{1\mathrm{trp}}$ in the one-triplon channel on the ground state for fixed one-triplon momentum k by writing

$$R^{S=1}|_{1\mathrm{trp}}|0\rangle=A_{1\mathrm{trp}}^{S=1}(k)|k\rangle, \tag{10}$$

where the amplitudes $A_{1\mathrm{trp}}^{S=1}$ are given by

$$A_{1\mathrm{trp}}^{S=1}=\frac{1}{\sqrt{2}}\sum_l\,[a_l^{\mathrm{L}}e^{-ik(2l+1/2)}+a_l^{\mathrm{R}}e^{-ik(2l-1/2)}]$$
$$=-\sqrt{2}i\sum_l\,a_l^L\sin\left[k\left(2l+\frac{1}{2}\right)\right]. \tag{11}$$

The sum runs over all strong bonds l. The coefficient a_l^L is the amplitude for the creation of one triplon at site l by S_L^z. The amplitudes of S_R^z do not need to be calculated separately due to the symmetry $a_l^R=-a_{-l}^L$. The basic unit length $a/2$ is the distance between two neighboring sites. In the figures momenta between 0 and 1 are given in units of $\pi/(a/2)$. So the comparison between our results and the conventional notation for undimerized chains using the distance $a'=a/2$ between two neighboring spins as unit length is simplified. In analytic expressions, the momenta k are given in units of $1/(a/2)$ (without the factor π) for brevity.

In Fig. 3 the results for the one-triplon dispersion $\omega(k)$ (left panels) and the one-triplon spectral weight $I_1(k)$ (right panels) are shown. We present results for $\lambda=\{0.3;0.4;0.5;0.6\}$ and $\alpha=0$ [Fig. 3(a)], $\alpha=0.25$ [Fig. 3(b)] and $\alpha=0.5$ [Fig. 3(c)].

Let us discuss first the case of vanishing frustration ($\alpha=0$). At $\lambda=0$ the system consists of isolated dimers and the one-triplon dispersion is flat. Turning on λ the triplon starts to hop from dimer to dimer and it acquires a finite dispersion [Fig. 3(a), left panel]. The dispersion has minima at $k=0$ and $k=\pi$ [in units of $1/(a/2)$], which represent the one-triplon gap Δ. In the limit of zero dimerization the one-triplon gap closes and it is to be expected that the one-triplon dispersion equals the well-known des Cloizeaux-Pearson[2] dispersion relation $\omega_{\mathrm{CP}}(k)=\pi/2|\sin(k)|$.

The one-triplon spectral weight $I_1(k)$ is shown in the right panel of Fig. 3(a). The leading term of $I_1(k)$ is proportional to $\sin^2(k/2)$. It is called the dimer structure factor.[50] The one-triplon spectral weight is concentrated at $k=\pi$. At finite dimerization the reduction of I_1 due to the interdimer exchange occurs mainly for momenta $k<0.9\pi$. The spectral weight increases in a small interval around $k=\pi$.[50] For even smaller dimerizations the one-triplon spectral weight becomes more concentrated about $k=\pi$. The total weight, integrated over momentum and frequency, vanishes for vanishing dimerization.

In Fig. 3(b) the corresponding results for $\alpha=0.25$ are shown. The one-triplon dispersion is similar in shape to the case of zero frustration. Due to the finite frustration the excitations become more local and the triplon is less dispersive. The gap values are slightly larger and the maximum values of the one-triplon dispersion are slightly lower for the various values of λ than for the unfrustrated case [Figs. 3(a) and 3(b), left panels].

The one-triplon spectral weight at $\alpha=0.25$ differs from the one at $\alpha=0$ for momenta close to $k=\pi$ [Fig. 3(b), right panel]. The spectral weight is reduced for all momenta at $\alpha=0.25$ on increasing λ. But the reduction is smallest for $k=\pi$. In the limit of zero dimerization the one-triplon spectral weight $I_1(k)$ vanishes for all momenta. The left panel of Fig. 3(c) shows the one-triplon dispersion $\omega(k)$ for $\alpha=0.5$. The

dispersion is highly reduced due to the increased locality of the triplon. At $k=\pi/2$, the one-triplon state is an eigen state of the system[52,53] and it has an energy of J independent of λ. In the limit of zero dimerization the system remains in a gapped state.[1,23–25,29]

The right panel of Fig. 3(c) shows $I_1(k)$ for $\alpha=0.5$. The spectral weight is reduced for increasing λ for all momenta except $k=\pi/2$. Since the one-triplon state at $k=\pi/2$ is an eigen state independent of λ its spectral weight is also constant.[54] In contrast to the previous cases, there is also a one-triplon contribution for zero dimerization, at least for $k=\pi/2$, but most probably also in the vicinity of this momentum.

B. Two-triplon contribution

In this section we discuss the two-triplon contribution to the dynamical structure factor. The two-triplon contribution displays additional physics in comparison to the one-triplon part. The reason is that besides the kinetic part of the excitations also the triplon-triplon interaction is important and has to be included. An attractive interaction can lead to bound states of two triplons. Furthermore, the total momentum of two triplons does not fix the state of the system. There is also a relative momentum between the triplons which is not fixed. Thus there is a continuum of two-triplon states for each given total momentum. Let us turn to the spectral properties of the two-triplon continuum and the two-triplon bound states.

We decompose the action of the full observable $R^{S=1}|_{2\mathrm{trp}}$ in the two-triplon channel on the ground-state for fixed two-triplon momentum k

$$R^{S=1}|_{2\mathrm{trp}}|0\rangle=\sum_d A^{S=1}_{2\mathrm{trp}}(k,d)|k,d\rangle. \tag{12}$$

Here d denotes the relative distance between the two triplons and

$$A^{S=1}_{2\mathrm{trp}}(k,d)=-\sqrt{2}i\sum_l a^{L,S=1}_{l,l+d}\sin\left[k\left(2l+\frac{1}{2}+d\right)\right]. \tag{13}$$

The sum runs over all strong bonds l and $a^{L,S=1}_{l,l+d}$ is the amplitude for the creation of two triplons on dimers l and $l+d$ by S^z_L. Here it is convenient to use a mixed representation in which the center-of-mass coordinate is Fourier transformed and the relative coordinate is dealt within real space. The action of S^z_R does not need to be calculated due to the relation $a^{R,S=1}_{l,l+d}=-a^{L,S=1}_{-l-d,-l}$. The basic unit length $a/2$ is again the distance between two neighboring sites. The spectra show results for momenta between 0 and 1 in units of $\pi/(a/2)$ (see Fig. 2). In Figs. 4–7 the results for the two-triplon continua, the dispersions of the two-triplon bound states and their spectral weights are shown.

Figure 4 displays the spectral density of the two-triplon continuum as a function of frequency and momentum. The spectrum for fixed momentum k is shifted by k in y direction in order to provide a three-dimensional view on the spectral densities. The lower and upper band edge is marked by solid gray lines. If there are any two-triplon bound states, their dispersions are displayed as a black lines. We denote the $S=1$ two-triplon bound states as T_n and the $S=0$ two-triplon bound states as S_n where $n=\{1,2,\ldots\}$.

Detailed information about the bound states is given in Fig. 5 which consists of two parts for each parameter set. The left part shows an enlargement of the dispersion of the bound state and of the lower bound of the two-triplon continuum. In the right part the corresponding spectral weight of the bound states is shown. The spectral weight is multiplied by the given factors for clarity.

What are the general features of the obtained spectra? Due to the conservation of the total S^z component there is no spectral weight at zero momentum. The energies of the system possess a reflection symmetry about $k=\pi/2$ which is a consequence of the inversion symmetry $k\leftrightarrow -k$ and of the coupling of the momenta k and $k+\pi$.[33] This symmetry can be seen clearly in the bound-state energies and in the lower and the upper band edges of the continuum. It does *not* hold for the spectral weights.[33]

In Fig. 4(a) the spectral density for $\lambda=0.3$ and $\alpha=0.0$ is shown. The spectral weight is mostly concentrated at the lower band edge of the continuum. There are two bound states centered about $k=\pi/2$ leaving the continuum at some finite momentum. The dispersions and the spectral weights of the bound states are plotted in Fig. 5(a). The points where the bound states are leaving the continuum can also be discerned by the strong peak close to the lower band edge of the continuum. The spectral weight is mainly concentrated in the first bound state T_1. The spectral weight of the second bound state T_2 is highly reduced.

The binding energy of the bound states has its maximum at $k=\pi/2$. It vanishes quadratically $\propto(k-k_c)^2$ when the

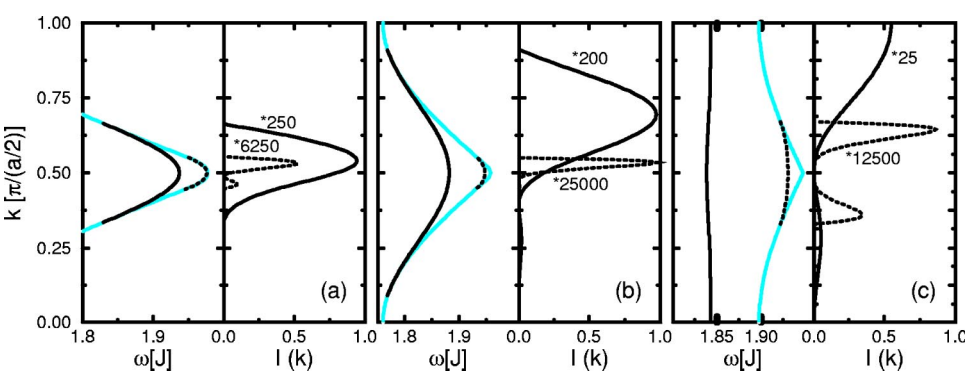

FIG. 5. Two-triplon bound states for $R^{S=1}$ with $\lambda=0.3$ and $\alpha=0.0$ (a), $\alpha=0.25$ (b), and $\alpha=0.5$ (c). Left panels show the dispersion of the bound states; right panels show the spectral weights of the bound states multiplied by the indicated factors. Gray lines denote lower bound of the continuum.

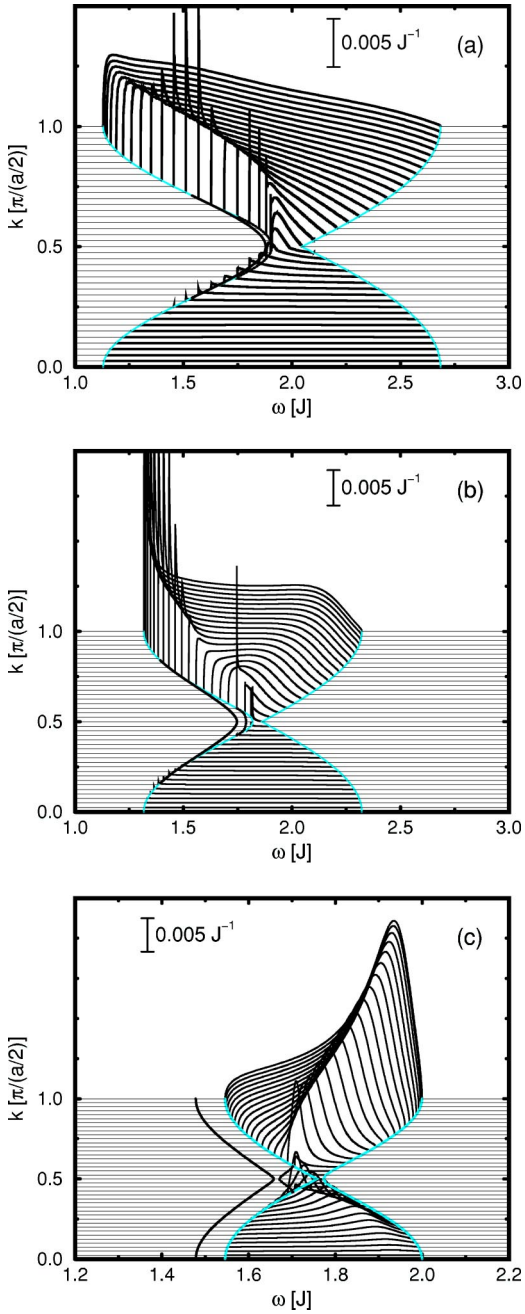

FIG. 6. Two-triplon spectral density $I_2(k,\omega)$ for $R^{S=1}$ with $\lambda=0.6$ and $\alpha=0.0$ (a), $\alpha=0.25$ (b), and $\alpha=0.5$ (c). Gray lines denote lower and upper bound of the continuum. Black lines indicate dispersion of two-triplon bound states.

bound state enters the continuum. Correspondingly their spectral weight vanishes linearly $\propto|k-k_c|$ in accordance with the exemplary calculation provided in Ref. 22. There it was shown for square-root-type continua that the binding energy vanishes quadratically as function of an external parameter while the spectral weight of the bound state vanishes linearly. The external parameter was the attraction strength. In the present case it is the total momentum which controls the relative strength of interaction and kinetic energy.

Decreasing the dimerization to intermediate values [$\lambda=0.6$, see Figs. 6(a) and 7(a)], there are no qualitative changes in the spectrum. The spectral weight is mainly concentrated at low energies. The range of energies, where the bound states exist, is slightly enhanced while the binding energy is slightly reduced. We expect that this tendency continues to lower values of the dimerization. For exactly zero dimerization, but *not* for an arbitrarily small but finite one, the first bound state T_1 coincides with the lower bound of the continuum leading to a square-root divergence at the lower edge of the continuum for all momenta. Our expectation is strongly corroborated by the exact results for the spectral densities in the sine-Gordon model.[34,55] The generic behavior is a square-root behavior at the band edges. Only if a breather becomes degenerate with the multi-particle band edge the square-root behavior switches to a square-root divergence. Exactly the same characteristics appears naturally in the triplon description. Recall also that for the uniform spin chain at zero dimerization the square-root divergence is well known from the exact two-spinon contribution to the dynamical structure factor.[4]

In Figs. 4(b) and 4(c) the spectra for strong dimerization and finite frustration $\alpha=0.25$ and $\alpha=0.5$ are shown. The corresponding information about the two-triplon bound states is plotted in Figs. 5(b) and 5(c). The frustration makes the excitations more local and less dispersive which leads to a narrowing of the two-triplon continuum. At the same time the triplon-triplon interaction is enhanced causing an increase of the binding energy of the bound states. It can be nicely seen that for $\alpha=0.25$ the first bound state extends over a wide range in momentum space lying for small and large momenta very close to the lower band edge inside the continuum. For $\alpha=0.5$ the bound state T_1 exists for all momenta.

Due to the existence of the bound states only in a finite interval of momentum for both values $\alpha=0$ and $\alpha=0.25$ the qualitative distribution of their spectral weight is similar. This is true for all values of frustration between 0 and 0.25. The same holds for the bound state T_2 for $\alpha=0.5$. In contrast, the spectral weight of the first bound state T_1, which is well separated from the continuum for $\alpha=0.5$, has its maximum at $k=\pi$.

The whole two-triplon contribution, i.e., the two-triplon bound states and the two-triplon continuum, vanishes for $k=\pi/2$ at $\alpha=0.5$. Here the one-triplon excitation is an exact eigen-state of the spectrum and therefore comprises the total spectral weight[52,53] (see also preceding section).

We now turn to the influence of the frustration on the *shape* of the two-triplon continuum. In the case of vanishing frustration the spectral weight is distributed mainly close to the lower band edge for strong and intermediate dimerization. The spectral weight decreases monotonically for higher energies. Turning on the frustration we observe a shift of spectral weight towards higher energies. In the case of strong dimerization this tendency is weak [Figs. 4(b) and 4(c)] while for intermediate dimerization we observe a huge transfer of spectral weight [Figs. 6(b) and 6(c)]. This transfer produces a non-monotonic shape for intermediate dimerization and $\alpha=0.25$, having a minimum of spectral weight inside the continuum [Fig. 6(b)]. Increasing the frustration (α

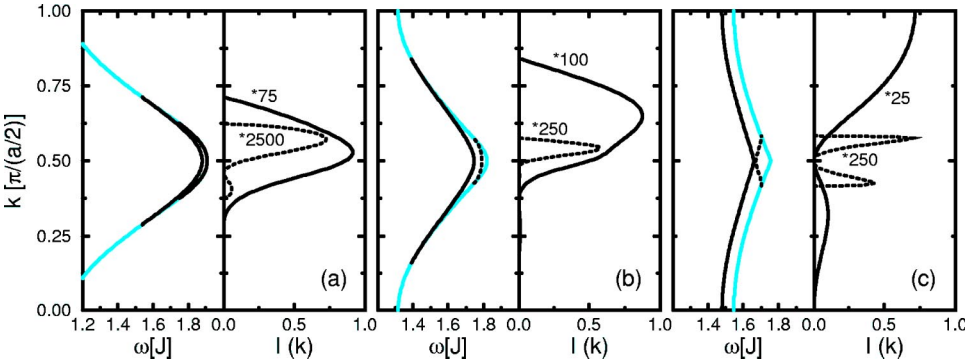

FIG. 7. Two-triplon bound states for $R^{S=1}$ with $\lambda=0.6$ and $\alpha=0.0$ (a), $\alpha=0.25$ (b), and $\alpha=0.5$ (c). Left panels show the dispersion of the bound states; right panels show the spectral weights of the bound states multiplied by the indicated factors. Gray lines denote the lower bound of the continuum.

$=0.5$) shifts the minimum to the lower band edge. The spectral weight is mainly at the upper band edge [Fig. 6(c)].

These observations are very similar to the results obtained by exact diagonalization at finite temperatures for the dynamical structure factor of a homogeneous spin chain including frustration.[51] There a decrease of spectral weight at $k=\pi$ inside the continuum is observed on increasing the frustration. This results in a high-energy maximum for large frustration and a minimum inside the continuum, i.e., a troughlike shape. From this comparison we conclude that our findings represent the generic features which are also valid in the limit of vanishing dimerization.

C. Comparison with field-theory results

In the first part of this section we concentrate on the $S=1$ breather and the corresponding behavior of the lower band edge of the two-triplon continuum. In the second part we have a closer look at the energy of the $S=0$ breather and at the one-triplon gap. Finally, the importance of marginal terms for the quantitative shape of spectral densities is discussed. A detailed analysis of the $S=0$ channel which contains also a discussion of the singlet two-triplon bound states is presented in the following section.

Let us first look at the results obtained from bosonization and the continuum limit renormalization group approach.[56,57] The bosonized form of the dimerized and frustrated spin chain reads

$$H_{\mathrm{FT}}=\frac{v}{2\pi}\int_{-\infty}^{\infty}[K(\pi\Pi)^2+K^{-1}(\partial_x\Phi)^2]dx + \int_{-\infty}^{\infty}[\delta A\cos(2\Phi)+D\cos(4\Phi)]dx, \qquad (14)$$

where v is the spin-wave velocity and $K=1/2$ the interaction parameter for the isotropic chain. The value of the critical frustration $\alpha_{0,c}=0.241\,167$ depends on the physics at short distances and is only accessible by numerical techniques.[12,23–25] The $\delta\cos(2\Phi)$ term is strongly relevant while the $D\cos(4\Phi)$ term is marginally irrelevant for $\alpha_0<\alpha_{0,c}$ and marginally relevant for $\alpha_0>\alpha_{0,c}$. It is commonly accepted and numerically confirmed[30,37,58,59] that the marginal term can be neglected best for $\alpha_0=\alpha_{0,c}$ (for further discussion see below). Then a simple sine-Gordon model at $K=1/2$ remains of which the spectral densities are known.[34,55]

The $S=1$ response function displays a square root divergence $\propto(\omega-\omega_0)^{-1/2}$ at the lower band edge. Here the energy of the $S=1$ breather $\omega_{\mathrm{br},S=1}$ is exactly degenerate with the lower band edge ($\omega_{\mathrm{br},S=1}=2\Delta$). This is in agreement with what we find at $\alpha=0.25$, cf. Figs. 4(b) and 6(b). Without any frustration, however, we find a square-root behavior $\propto(\omega-\omega_0)^{1/2}$, cf. Figs. 4(a) and 6(a). Hence we conclude that the sine-Gordon model does not describe the unfrustrated, dimerized spin chain exhaustively. But the sine-Gordon model applies to the spin chain at critical frustration where the higher cosine-term $\cos(4\Phi)$ vanishes. It is interesting to note that we find a square-root divergence for $\alpha\approx\alpha_{0,c}$ and not for $\alpha_0\approx\alpha_{0,c}$.

The conclusion about the applicability of the sine-Gordon model to the unfrustrated and dimerized spin chain is in agreement with the results of the numerical investigation of the bound states.[37] It is known that the elementary excitations of the SU(2) symmetric sine-Gordon model consist of soliton and antisoliton excitations and two breathers, bound states, plus one breather which is degenerate with the lower band edge.[1,33,60] The lowest-lying breather is degenerate with the soliton and antisoliton excitations and corresponds to the $S^z=0$ triplet state in spin language. This fixes the interaction

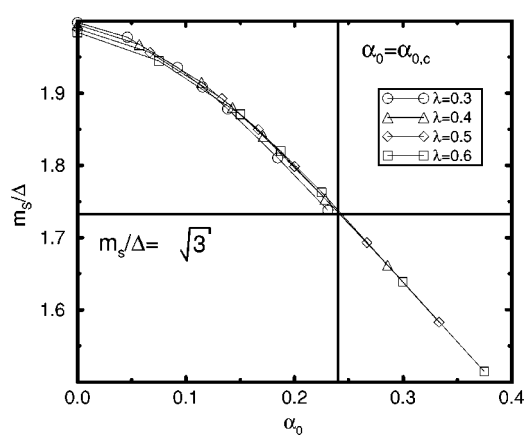

FIG. 8. Ratio of the singlet two-triplon bound state energy m_S over the one-triplon gap Δ for $\lambda=\{0.3;0.4;0.5;0.6\}$ depending on the frustration α_0. Horizontal black solid line denotes $\sqrt{3}$ and vertical black solid line shows the critical frustration $\alpha_{0,c}$.

parameter to $K=1/2$. The second breather is assigned to a spin singlet excitation, since there is no counter part in the soliton or antisoliton sector. The ratio between the energy of the $S=0$ breather $\omega_{\mathrm{br},S=0}$ and the one-triplon gap Δ is exactly $\sqrt{3}$ at $K=1/2$.

In Fig. 8 this ratio is shown for various values of $\lambda=\{0.3;0.4;0.5;0.6\}$ versus the bare frustration α_0. We have used Padé extrapolants for $\lambda=0.6$. It can be clearly seen that almost all points (except the case for strong dimerization $\lambda=0.3$) fall onto one curve. The values for $\alpha_{0,c}$ and $\sqrt{3}$ are included as solid lines. The point where these two lines cross lies on the calculated curve and corresponds to the prediction of the SU(2) symmetric sine-Gordon model. In all other cases ($\alpha_0\neq\alpha_{0,c}$) the ratio $\omega_{\mathrm{br},S=0}/\Delta$ differs from $\sqrt{3}$. This is due to corrections resulting from the marginal term $\cos(4\Phi)$. Our calculations agree perfectly with previous numerical results.[37]

The relative importance of the two cosine terms in Eq. (14) at finite dimerization is a subtle issue which we discuss in the following.

In the self-consistent harmonic approximation[61,62] we replace $\Phi\rightarrow\Phi_{\mathrm{class}}+\hat{\Phi}_{\mathrm{fluct}}$ where only the fluctuation part is of operator character. The cosine terms can then be approximated by

$$\cos(n\Phi)\rightarrow\exp[-(n^2/2)\sigma(x)]\cos[n\Phi_{\mathrm{class}}(x)]\times\left(1-\frac{n^2}{2}\hat{\Phi}^2_{\mathrm{fluct}}\right). \tag{15}$$

where $\sigma(x):=\langle\hat{\Phi}_{\mathrm{fluct}}(x)^2\rangle$. This kind of approach corresponds to renormalization in first order. In the ground state (without solitons) one has $\Phi_{\mathrm{class}}=0$. In the ungapped phase the fluctuations diverge, hence $\sigma\rightarrow\infty$. But in the gapped phase, the fluctuations are cut off at low energies so that $\sigma=-(K/2)\ln(\Delta/\Delta_0)$ where Δ is the gap and Δ_0 is proportional to the ultraviolet cutoff.

Since the square of the gap Δ^2 is proportional to the coefficient of $\hat{\Phi}(x)^2$ one obtains from the term $\delta\cos(2\Phi)$ the self-consistency equation

$$\Delta^2\propto\delta\exp(-2\sigma), \tag{16a}$$

$$\Delta\propto\delta^{1/(2-K)}, \tag{16b}$$

yielding the well known $\Delta\propto\delta^{2/3}$ by Cross and Fisher.[63] Hence the total contribution of this cosine-term is proportional to Δ^2 or $\delta^{4/3}$. The crucial point to note is that the amplitude of the second cosine-term $\cos(4\Phi)$ is of the same magnitude $\exp(-8\sigma)\propto\Delta^{4K}$ which also yields Δ^2 or $\delta^{4/3}$ for $K=1/2$.[65] Hence the self-consistent harmonic approximation tells us that even in the regime where the frustration is marginally irrelevant $\alpha<\alpha_c$ it influences the low-energy physics on the quantitative level.

Considering, however, the renormalization to second order the marginally irrelevant term is reduced logarithmically, hence the name "marginally irrelevant" (Refs. 34,64). The flow is valid down to the infrared cutoff which is in our case the energy gap due to dimerization. Note that we are working in the thermodynamic limit $L=\infty$. Hence the suppression of the marginally irrelevant cosine term relative to the relevant one is logarithmic in δ and so very slow. Thus it is possible that the scales which we discuss in this paper (δ down to 0.25) are still too large to see the emergence of the physics of a pure sine-Gordon model with one cosine only. But we find it puzzling that no precursors of the convergence to the predictions of the pure sine-Gordon model can be seen. The ratio of the energy gaps shown in Fig. 8 (or those obtained in Ref. 37) appears almost independent of δ as far as we could investigate.

Note that the vanishing of the $\cos(4\Phi)$ term at the *end* of the flow of l is *not* identical to the question whether this term is present at the beginning of the flow. We presume that this difference explains the puzzling finding that the bare coefficient of the Umklapp term $\cos(4\Phi)$ vanishes[1] at $\alpha_0=1/6$, that means relatively far from the quantum critical point $\alpha_0=0.241$.

Our results in Figs. 4–6(a,b) show that the square-root divergence known from the sine-Gordon model[34,55] is changed to normal square-root behavior. So the quantitative changes of the low-energy Hamiltonian influence the shape of the spectral densities qualitatively. Hence for spectral densities one must know whether the appropriate effective low-energy model is a (simple) sine-Gordon model or a double sine-Gordon model with two cosine terms. The answer depends on the energy scale considered, i.e., the value of δ.

For strong frustration $\alpha=0.5$, cf. Figs. 4(c) and 6(c), the physics is dominated by bound states. Their number proliferates for decreasing dimerization.[65,66] At $\delta=0$ there are infinitely many bound states densely distributed between Δ and 2Δ. They form the continuum which can be understood as two-spinon continuum.[29,65,66] The values of λ for which we display the spectral densities in Figs. 4(c) and 6(c) are still too low, i.e., too far in the dimerized regime to see more than two bound states. This was also observed by Zheng *et al.*[67] They found in a series expansion up to order λ^{19} three singlet and three triplet bound states.

We attribute the fact, that only a small number of bound states could be found so far, to the limited range of the effective interaction. In the perturbative approaches for $\alpha=0.5$ an order of λ^n corresponds to a maximum range of $[n/2]$. So even calculations at $n=19$ provide only a potential of small finite range which does not allow for many bound states. The alternative presumption[67] that the lacking bound states are found in the channels with more than two triplons would require that the spectral weight is passed to channels with more and more triplons. No channel with only a finite number of bound states may retain a finite spectral weight at zero dimerization since at zero dimerization only a continuum is found.[29] None of our results is in favor of this scenario so that we are convinced that the range of the interaction is the crucial point. The fact that an expansion to higher order finds more bound states in the two-triplon sector supports the view that the range of the interaction matters. But the precise description of the deconfinement transition for vanishing dimerization is still an open issue. Future developments like self-similar realizations of the continuous

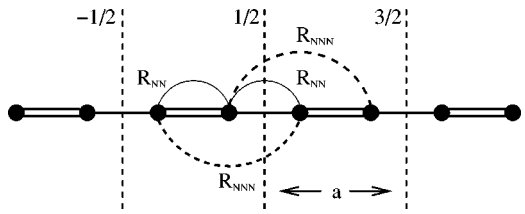

FIG. 9. Sketch of the local observables for $S=0$ excitations. $R_{\mathrm{NN}}^{S=0}$ is a sum of couplings on strong bonds (double lines) and weak bonds (single line). $R_{\mathrm{NNN}}^{S=0}$ couples next nearest neighbor spins.

unitary transformations will help to release this constraint on the range of the interaction.[46,68]

Concerning the present data at strong frustration, an important trend is that on increasing λ the spectral weight is shifted towards higher energies.

V. $S=0$ EXCITATIONS

In this section we concentrate on the two-triplon contribution to the spectral density with total spin zero which is relevant for optical experiments. For $S=0$ one needs at least two triplons which form together a state with vanishing total spin. For the case of isolated dimers ($\lambda=0$) the total spectral weight is in the two-triplon contribution. At finite λ the spectral weight in the two-triplon channel is reduced and spectral weight is also found in channels with more than two triplons.

In the limit of vanishing dimerization for zero frustration we can show in a similar analysis as for the dynamical structure factor that the two-triplon contribution possesses almost the total spectral weight.[22] The two-triplon contribution is therefore the only sizable contribution for the whole range of dimerizations for the unfrustrated case. In presence of frustration the analogous analysis is quantitatively more difficult as stated before. But there are again indications that only a small number of triplons dominates the spectral properties. Therefore, we investigate the leading two-triplon contribution for the $S=0$ channel. For the dimerizations treated in this work there is no doubt that the two-triplon contribution is the only sizable term. The crucial point, however, is to which extent we can obtain the generic features which govern also the limit of vanishing dimerization. All results obtained so far show that the one- and two-triplon contributions capture indeed the relevant physics.

The local physical observable $R^{S=0}$ for $S=0$ excitations reads

$$R_{\mathrm{loc}}^{S=0}=R_{\mathrm{loc,NN}}^{S=0}+\beta R_{\mathrm{loc,NNN}}^{S=0}, \tag{17}$$

i.e., it is a sum over NN and NNN. The coefficient β is a measure for the relative strength between the two couplings. It depends on the underlying microscopic physics and will not be discussed in this work. As illustrated in Fig. 9 these observables are given by

$$R_{\mathrm{loc,NN}}^{S=0}=(1+\gamma)\mathbf{S}_{0,\mathrm{L}}S_{0,\mathrm{R}}+(1-\gamma)\mathbf{S}_{0,\mathrm{R}}S_{1,\mathrm{L}} \tag{18}$$

for NN coupling, and

$$R_{\mathrm{loc,NNN}}^{S=0}=\mathbf{S}_{0,\mathrm{L}}\mathbf{S}_{1,\mathrm{L}}+\mathbf{S}_{0,\mathrm{R}}\mathbf{S}_{1,\mathrm{R}} \tag{19}$$

for NNN coupling where γ is proportional to the dimerization δ. $R_{\mathrm{loc,NN}}^{S=0}$ is a sum over couplings on weak and strong bonds.

We will restrict our discussion to the case of NN coupling on the weak bonds and on the NNN coupling. This choice is motivated by the relevance of various observables for Raman spectroscopy and infrared absorption in the limit of vanishing dimerization. Raman spectroscopy measures excitations with total momentum zero while infrared absorption is governed by the response at large momenta.[69,70]

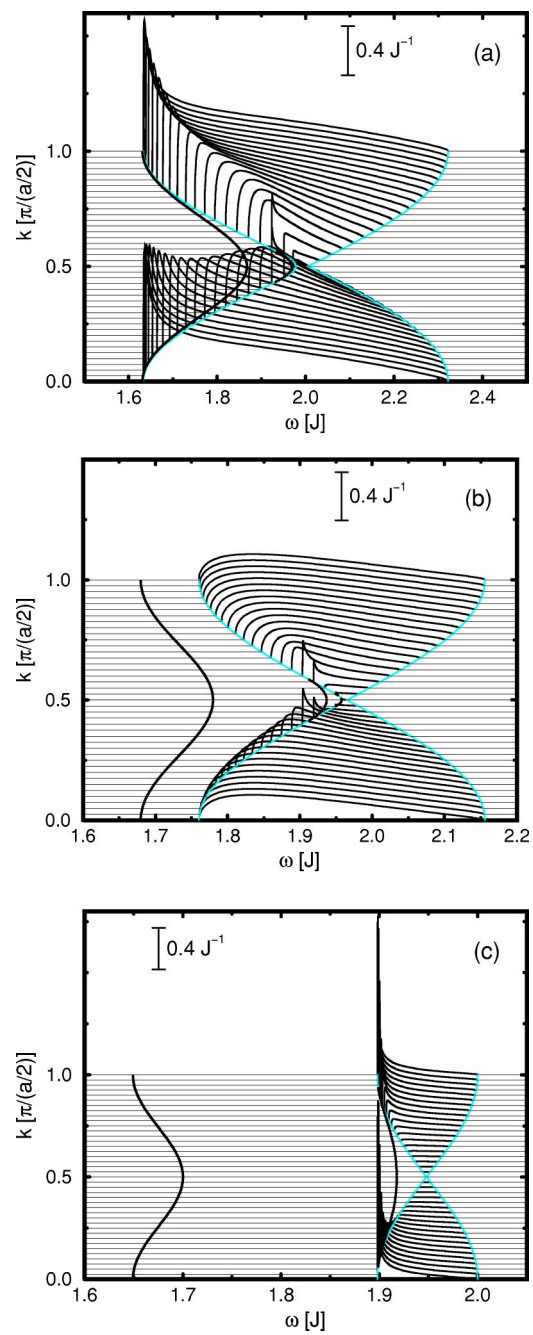

FIG. 10. Two-triplon spectral density $I_2(k,\omega)$ for $R_{\mathrm{NN,weak}}^{S=0}$ with $\lambda=0.3$ and $\alpha=0.0$ (a), $\alpha=0.25$ (b), and $\alpha=0.5$ (c). Gray lines denote lower and upper bound of the continuum. Black lines indicate dispersion of two-triplon bound states.

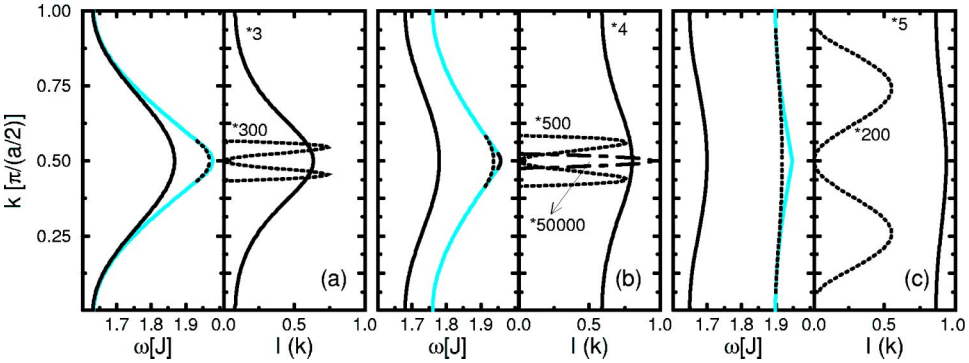

FIG. 11. Two-triplon bound states for $R^{S=0}_{\mathrm{NN,weak}}$ with $\lambda=0.3$ and $\alpha=0.0$ (a), $\alpha=0.25$ (b), and $\alpha=0.5$ (c). Left panels show the dispersion of the bound states; right panels show the spectral weights of the bound states multiplied by the indicated factors. Gray lines denote lower bound of the continuum.

In the case of a uniform spin chain without frustration the NN Raman operator commutes with the Hamiltonian and one obtains a vanishing Raman response. Therefore the NNN Raman operator is the leading contribution in terms of a Loudon-Fleury scattering theory.[71,72] In contrast, R_{NN} does not commute for finite momenta with the Hamiltonian and will be the most important contribution to the infrared absorption. For simplicity, we do not treat R_{NN} completely but only the weak-bond part. This is no major restriction because we are interested in the generic properties of these quantities. In addition, the weak-bond part dominates for strong dimerization.

We will discuss the two observables R_{NN} and R_{NNN} separately. For a direct comparison with experimental data one should take the sum over all contributing parts of $R^{S=0}(k)$ to account for possible interference effects. The necessary superposition, however, depends strongly on the details of the system and cannot be discussed generally.

The action of the full observable on the ground state is decomposed again for fixed total momentum k in the two-triplon sector by

$$R^{S=0}_{\mathrm{NN,weak}}(k)|0\rangle=\sum_d A^{S=0}_{\mathrm{2trp,NN,weak}}(k,d)|k,d\rangle \tag{20a}$$

$$R^{S=0}_{\mathrm{NNN}}(k)|0\rangle=\sum_d A^{S=0}_{\mathrm{2trp,NNN}}(k,d)|k,d\rangle, \tag{20b}$$

where

$$A^{S=0}_{\mathrm{2trp,NN,weak}}(k,d)=\sqrt{2}\sum_l a^{\mathrm{weak,NN}}_{l,l+d}\cos[k(2l+d)] \tag{21a}$$

$$A^{S=0}_{\mathrm{2trp,NNN}}(k,d)=\sqrt{2}\sum_l a^{\mathrm{L,NNN}}_{l,l+d}\cos[k(2l+1/2+d)]. \tag{21b}$$

Here d is the distance between the two triplons, $a^{\mathrm{weak,NN}}_{l,l+d}$ is the amplitude for the creation of two triplons on the dimers l and $l+d$ by $\mathbf{S}_{0,\mathrm{R}}\mathbf{S}_{1,\mathrm{L}}$, and $a^{\mathrm{L,NNN}}_{l,l+d}$ is the amplitude for the creation of two triplons on the dimers l and $l+d$ by $\mathbf{S}_{0,\mathrm{L}}\mathbf{S}_{1,\mathrm{L}}$. It is not necessary to calculate $a^{\mathrm{R,NNN}}_{l,l+d}$ due to the symmetry $a^{\mathrm{R,NNN}}_{l,l+d}=a^{\mathrm{L,NNN}}_{-l-d,-l}$. The basic unit length $a/2$ is again the distance between two neighboring sites. Momentum is measured in units of $\pi/(a/2)$.

We first discuss the symmetries of the two observables. $R^{S=0}_{\mathrm{NN,weak}}$ possesses a reflection symmetry about $k=\pi/2$ for the same reasons as the Hamiltonian. For any mode at k which is created by $R^{S=0}_{\mathrm{NN,weak}}$ there is also a mode at $k+\pi$ which is created. In addition, each mode at k is degenerate with the reflected mode at $-k$. Therefore, the whole spectral density will be symmetric about $k=\pi/2$. This symmetry is absent for $R^{S=0}_{\mathrm{NNN}}$. For $R^{S=0}_{\mathrm{NNN}}$ the spectral weight is mainly concentrated at small and intermediate momenta while it vanishes exactly at $k=\pi$. The latter follows from the fact that at $k=\pi$ the observable creates an odd state with respect to reflection about the axis 1/2 (see Fig. 9) while a singlet made from two triplets is always an even state with respect to particle exchange.

In Figs. 10–13 the spectral densities for $R^{S=0}_{\mathrm{NN,weak}}$ are shown and in Figs. 14–17 the corresponding densities for $R^{S=0}_{\mathrm{NNN}}$. First we discuss the results for the NN coupling $R^{S=0}_{\mathrm{NN,weak}}$ passing then to the results for NNN coupling $R^{S=0}_{\mathrm{NNN}}$. Finally, the implications for Raman spectroscopy and infrared absorption will be assessed.

A. Case: $R^{S=0}_{\mathrm{NN,weak}}$

In Fig. 10(a) the spectral density for strong dimerization ($\lambda=0.3$) and vanishing frustration is depicted. The corresponding information about the dispersion and the spectral weight of the two-triplon bound states is shown in Fig. 11(a). The same notation as in the section for $S=1$ excitations is used. The spectrum is symmetric about $k=\pi/2$ due to the inversion symmetry $k\leftrightarrow -k$ and $R^{S=0}_{\mathrm{NN,weak}}(k+\pi)=R^{S=0}_{\mathrm{NN,weak}}(k)$.

We find two $S=0$ two-triplon bound states S_1 and S_2. The triplon-triplon interaction is larger in the total $S=0$ channel than it was in the total $S=1$ channel. Therefore the binding energy of the bound states is enhanced and the first bound state S_1 exists for all momenta in contrast to the $S=1$ case. In general, the $S=0$ channel is dominated by the bound states which carry most of the spectral weight. This statement applies also to the experimental relevance, see below.

The dispersion of the two-triplon bound state S_1 is roughly sinusoidal having three extrema at momenta $k=\{0;\pi/2;\pi\}$. The binding energy is largest for $k=\pi/2$ while it becomes small near momentum zero and π. The spectral weight of S_1 is roughly proportional to the binding energy. The second singlet two-triplon bound state S_2 exists only in

a finite interval about $k=\pi/2$. The spectral weight of S_2 vanishes at $k=\pi/2$ and possesses two maxima below and above $k=\pi/2$.

The spectral weight of the two-triplon continuum is concentrated at small frequencies. At small and large momenta this effect is enhanced due to the vicinity of S_1. Lowering the dimerization we see no qualitative changes in comparison to the case of strong dimerization [Figs. 12(a) and 13(a)]. So we expect that the dispersion of the bound state S_1 is degenerate with the lower band edge of the two-triplon continuum inducing a square-root divergence. This expectation is supported also by numerical results for the second breather.[37]

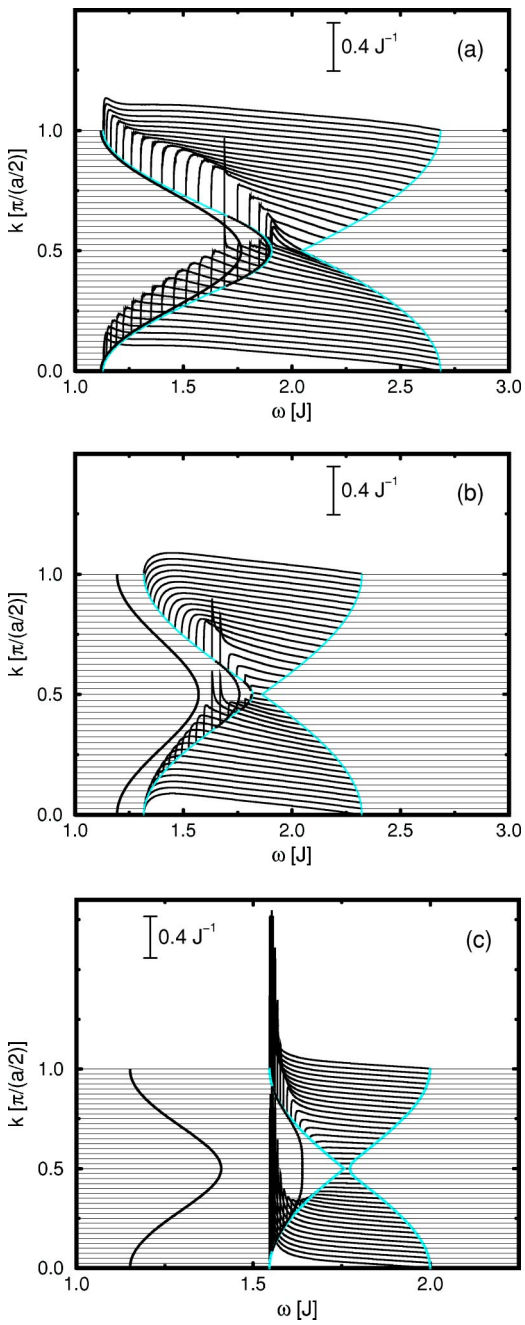

FIG. 12. Two-triplon spectral density $I_2(k,\omega)$ for $R^{S=0}_{\mathrm{NN,weak}}$ with $\lambda=0.6$ and $\alpha=0.0$ (a), $\alpha=0.25$ (b), and $\alpha=0.5$ (c). Gray lines denote lower and upper bound of the continuum. Black lines indicate dispersion of two-triplon bound states.

For clarity, we like to emphasize again that one must clearly distinguish the case of zero dimerization and the case of small, but finite, dimerization. For zero dimerization bosonization predicts a $1/\omega$ divergence at $k=\pi$ which becomes $(\omega-\omega_0)^{-1/2}$ close to $k=\pi$.[1,63] This has been used, for instance, in the empirical calculation of Lorenzana and Eder.[74] For small, but finite, dimerization the sine-Gordon model prediction of a square-root behavior without divergence applies to the critical frustration and in the region around this value. For other values of the frustration a breather may coincide with the lower band edge implying a square-root divergence.

In Figs. 10(b) and 10(c) the spectral density at finite frustration for strong dimerization is shown. At $\alpha=0.25$ we find three bound states S_1, S_2, and S_3. The binding energy of S_1 increases drastically on turning on the frustration, especially at small and large momenta. The spectral weight increases in a similar fashion for these momenta. The third two-triplon bound state S_3 exists merely in a very small region about $k=\pi/2$. The binding energy and the spectral weight are tiny. The spectral weight has a maximum at $k=\pi/2$.

The two-triplon continuum for $\alpha=0.25$ does not show much structure. This is a consequence of the fact that at almost all momenta no bound state is close to the lower band edge of the continuum. On decreasing the dimerization, no qualitative changes are seen [see Fig. 12(b)].

At $\alpha=0.5$ we detect two bound states. The dispersion of S_1 becomes flatter which holds also for the spectral weight distribution. The biggest change can be seen in S_2. This bound state exists for almost all momenta in contrast to the cases $\alpha=\{0;0.25\}$. In the regions close to $k=0$ and symmetrically close to $k=\pi$, the bound state S_2 does not exist, but it can be thought to lie just above the lower band edge implying an almost divergent behavior of the two-triplon continuum.

Smirnov[34,55] showed that the corresponding spectral density of the sine-Gordon model displays a square-root behavior at the lower band edge. This applies to the $S=0$ channel of the frustrated spin chain at $\alpha\leqq\alpha_{0,c}$ if the marginal term $D\cos(4\Phi)$ of Eq. (14) is neglected. This neglect is quantitatively justified for $\alpha=\alpha_{0,c}$. Indeed, our results clearly show a square-root behavior for $\alpha=0.25$. As for the $S=1$ case, we find that the predictions of the sine-Gordon model for the physics of the spin chain are verified for $\alpha=\alpha_{0,c}$. For other values, notably $\alpha=0$ and $\alpha=0.5$, we find square-root divergences or strong tendencies towards square-root divergences. Again, such divergent behavior results from the vicinity of bound states, here in the $S=0$ sector.

B. Case: $R^{S=0}_{\mathrm{NNN}}$

In Figs. 14 and 16 the spectral densities of the observable $R^{S=0}_{\mathrm{NNN}}$ for various values of dimerization and frustration are shown. The information on the singlet two-triplon bound states is plotted in Figs. 15 and 17. All considerations con-

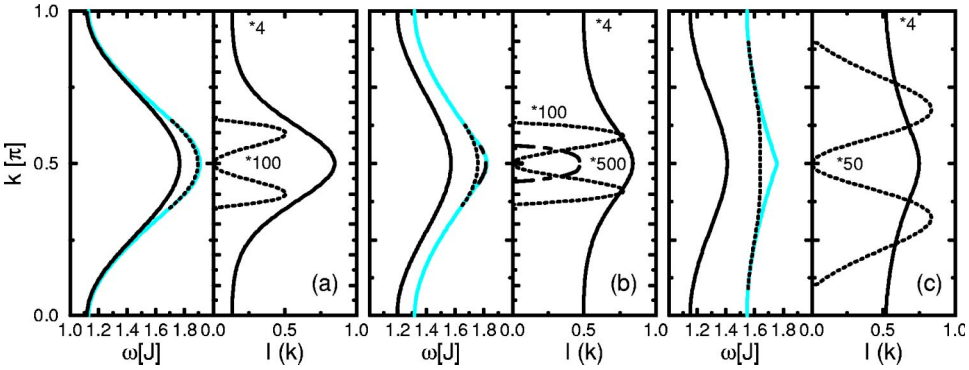

FIG. 13. Two-triplon bound states for $R^{S=0}_{\mathrm{NN,weak}}$ with $\lambda=0.6$ and $\alpha=0.0$ (a), $\alpha=0.25$ (b), and $\alpha=0.5$ (c). Left panels show the dispersion of the bound states; right panels the spectral weights of the bound states multiplied by the indicated factors. Gray lines denote lower bound of the continuum.

cerning the energetic properties of the $S=0$ channel are the same as for $R^{S=0}_{\mathrm{NNN}}$ and need not be discussed again in this section.

We concentrate on the spectral differences between the two observables. The spectral weight is suppressed for large momenta due to symmetry reasons. This can be clearly seen for the two-triplon continuum and the spectral weight of the two-triplon bound states. Therefore only momenta $k \in [0,\pi/2]$ carry significant spectral weight. In this region we do not find qualitative changes to the results for $R^{S=0}_{\mathrm{NN,weak}}$.

The most important difference is a change of the spectral weight distribution of S_1. At $\alpha=0$ the spectral weight has a maximum at $k=\pi/2$ which is similar to the case of $R^{S=0}_{\mathrm{NN,weak}}$. Finite frustration shifts the maximum to $k=0$. Close to the critical frustration the spectral weight is almost constant for $k\in[0,\pi/2]$. At $\alpha=0.5$ the spectral weight is a monotonically decreasing function (from $k=0$ to $k=\pi$).

C. Raman spectroscopy

The dominant observable for magnetic light scattering (Raman response) using the standard Fleury-Loudon scattering theory[71,72] is

$$R_{\mathrm{Raman}}=\sum_i\ [R^{S=0}_{\mathrm{loc,NN}}(i)+\beta R^{S=0}_{\mathrm{loc,NNN}}(i)], \tag{22}$$

where the sum runs over all spins. The Raman response is therefore the $k=0$ contribution to the spectral density as we have discussed in the preceding section. We focus here on the case of NNN coupling which is the leading process in the case of a uniform Heisenberg chain without frustration.

In Fig. 18 the Raman response for NN coupling is shown at zero frustration (a), close to critical frustration $\alpha=0.25$ (b) and for $\alpha=0.5$ (c). In each graph the spectrum is shown for $\lambda=\{0.3;0.4;0.5;0.6\}$. In these figures, a broadening of $\Gamma=0.01$ is used and the spectra are shifted in y direction for clarity. The spectral densities for $\alpha=0$ are multiplied by 6.

For the dimerizations considered here, the spectra are dominated by the first $S=0$ two-triplon bound state S_1. This dominance is enhanced by the frustration. In Fig. 18(a) the case of vanishing frustration is shown. Due to the finite broadening and the small binding energy of the bound state there is no separation of the two-triplon bound state and the two-triplon continuum. An increase of λ reduces the weight of the bound state and gives rise to a broad featureless continuum.

In Figs. 18(b) and 18(c) the results for finite frustration are plotted. The binding energy of the bound state S_1 is enhanced and one can clearly separate the contribution of the bound state S_1 and the continuum. The spectral weight of the two-triplon continuum is very small.

D. Infrared absorption

In this section we apply our results to phonon-assisted infrared absorption of magnetic excitations.[69,70] This technique allows to study the spin-spin correlation function by measuring the optical conductivity. The direct absorption of two magnetic excitations is generically not allowed due to inversion symmetry. However, this selection rule can be broken by simultaneously exciting a phonon. The leading infrared-active magnetic absorption is a two-triplon-plus-phonon process.[69,70] Due to the momentum of the excited phonon, the magnetic spectra $I(k,\omega)$ have to be integrated over all momenta weighted with a phonon-specific form factor.

The absorption spectra are sensitive to the $S=0$ two-triplon bound states. Especially the extrema yield prominent van-Hove singularities in the density of states which can be identified in experiment. In this way, the first experimental evidence for the two-triplon bound state in cuprate spin ladder systems[73] was possible. We therefore expect interesting line shapes also in the optical absorption also for dimerized and frustrated spin chain systems.

The absorption coefficient is given by[74]

$$a(\omega)=a_0\omega I^{\mathrm{IR}}(\omega-\omega_0). \tag{23}$$

Here a_0 is a constant depending on the material and ω_0 is the phonon frequency. The phonon is considered to be local and without dispersion. The function I^{IR} is given by

$$I^{\mathrm{IR}}(\omega)=16\pi\sum_k\ \sin^4(k/2)I(k,\omega). \tag{24}$$

The specific form factor given is strictly valid only for a uniform Heisenberg chain. It was successfully used to explain the optical absorption in uniform cuprate spin chains.[74,75] We use the same form factor also for the dimerized and frustrated chain in order to explore the general fea-

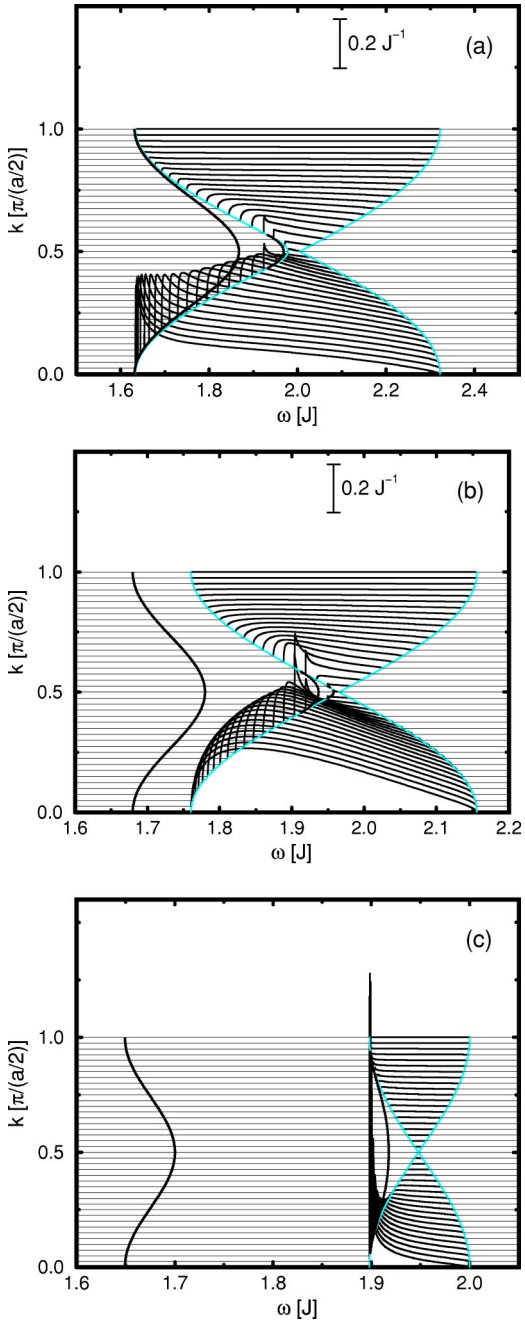

FIG. 14. Two-triplon spectral density $I_2(k,\omega)$ for $R^{S=0}_{\mathrm{NNN}}$ with $\lambda=0.3$ and $\alpha=0.0$ (a), $\alpha=0.25$ (b), and $\alpha=0.5$ (c). Gray lines denote lower and upper bound of the continuum. Black lines indicate dispersion of two-triplon bound states.

tures of the optical conductivity and to compare the line shapes at finite dimerization with the line shapes at zero dimerization. In a detailed analysis of experimental data one must analyze which phonons are involved and which specific form factors matter.

In Figs. 19(a)–19(c) and Figs. 20(a)–20(c) the optical absorption $a(\omega)$ for various dimerization and frustration is shown for $R^{S=0}_{\mathrm{NNN}}$ and $R^{S=0}_{\mathrm{NN,weak}}$. Here a_0 is set to one and ω_0 is set to zero. The spectra are plotted with a broadening of $\Gamma=0.01$ which is a reasonable value in view of experimental resolutions. In the insets we show the contribution of the two-triplon continuum without the broadening to highlight the shape of the continuum contributions and to distinguish it from contributions of the bound states.

The phonon form factor favors large momenta while it reduces the contribution of small momenta. Hence the discussion of the spectral densities implies that $R^{S=0}_{\mathrm{NN,weak}}$ is more relevant than $R^{S=0}_{\mathrm{NNN}}$ for $a(\omega)$. This can also be seen in the absolute heights of the spectra in Figs. 19 and 20. In addition, we expect that the NN coupling is stronger than the NNN one because exchange processes of longer range will generically be less important.

We start our discussion with $R^{S=0}_{\mathrm{NN,weak}}$. As stated above the first $S=0$ two-triplon bound state S_1 carries most of the spectral weight for all momenta. Hence, it is of crucial importance for the optical absorption. In Figs. 11 and 13, we show that the dispersion $\omega_{\mathrm{bound}}(k)$ of the bound state S_1 possesses three extrema at $k=\{0,\pi/2,\pi\}$. So we obtain three van-Hove singularities in $I^{\mathrm{IR}}(\omega)$. The spectral density is symmetric about $k=\pi/2$ so that two van-Hove singularities coincide and there are two peaks resulting from the bound state S_1 in the optical conductivity. The weight of the minimum at $k=0$ is suppressed by the phonon form factor. This implies that the regions about $k=\pi/2$ and $k=\pi$ dominate.

In Fig. 19(a) the optical absorption for a dimerized chain ($\lambda=\{0.3,0.3,0.5,0.6\}$) without frustration is depicted. The spectra are shifted in y direction for clarity. The line shape is dominated by a small peak at low energies, a sharp peak at intermediate energies and a broad structure at high energies. The first two features are mainly produced by the above mentioned van-Hove singularities resulting from the extrema of the bound state dispersion of S_1. The second peak is dominant because the spectral weight has a maximum for $k=\pi/2$, see Figs. 11(a) and 13(a). For increasing λ this peak looses intensity while the first peak becomes more pronounced. The latter effect is due to the increasing binding energy of S_1 at $k=\pi$.

For strong dimerization the feature at low energies, which is rather a shoulder than a peak, is an effect of the two-triplon continuum [inset of Fig. 19(a)]. The second bound state S_2 is of no greater relevance for the optical absorption because it has zero spectral weight for $k=\pi/2$ which is the only extremum of the bound-state dispersion. In addition, the binding energy is very small without frustration and so is the corresponding spectral weight.

Lorenzana and Eder[74] calculated the two-spinon-plus-phonon contribution to the optical absorption for a uniform Heisenberg chain. The line shape consists mainly of three parts: a concave uprise at low energies which vanishes for zero frequency, a singularity at intermediate energies, and a convex tail for higher frequencies. It is very interesting to see that all these features have precursors at finite dimerization which are captured in the triplon picture.

In the limit of vanishing dimerization, the system becomes gapless and the spectra therefore start at zero energy. As long as there is some finite dimerization the bound state S_1 exists and produces the concave uprise at small energies and the singularity at intermediate energies resulting from

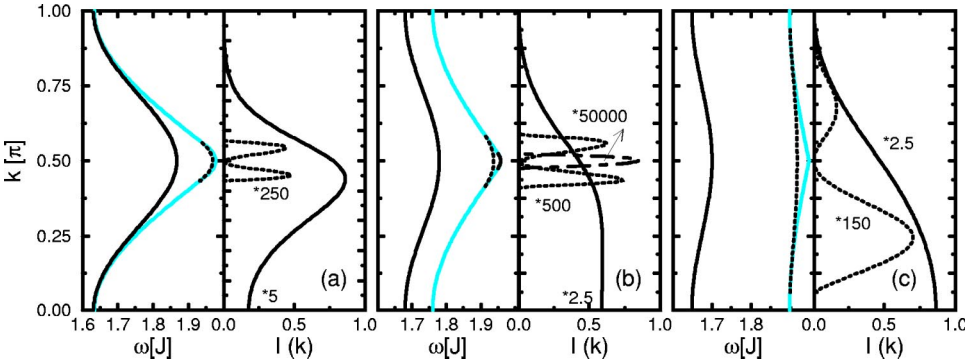

FIG. 15. Two-triplon bound states for $R_{\mathrm{NNN}}^{S=0}$ with $\lambda=0.3$ and $\alpha=0.0$ (a), $\alpha=0.25$ (b), and $\alpha=0.5$ (c). Left panels show the dispersion of the bound states; right panels show the spectral weights of the bound states multiplied by the indicated factors. Gray lines denote lower bound of the continuum.

the maximum at $k=\pi/2$. We expect that for vanishing dimerization ($\lambda=1$) the dispersion of S_1 coincides with the lower band edge of the two-triplon continuum leading to a square-root divergence at the lower band edge for all momenta. Since the dispersions and the band edges display an extremum at $k=\pi/2$ this divergence leads to the singularity discernible at intermediate energies. The convex tail at the upper band edge is equally present even for strongly dimerized chains, see inset in Fig. 19(a). It is a consequence of the convex square-root behavior at the upper edge of the two-triplon continuum.

In Figs. 19(b) and 19(c) the optical absorption at finite frustration $\alpha=0.25$ and $\alpha=0.5$ for the same value of dimerization is shown. As discussed earlier the frustration enhances the triplon-triplon interaction and increases the binding energy of the two-triplon bound states. As can be clearly seen in Figs. 11(b) and 11(c) and Figs. 13(b) and 13(c) the spectral weight of S_1 at $k=\pi$ increases compared to the weight at $k=\pi/2$. Therefore, the first peak in the optical absorption becomes more and more prominent on increasing frustration. This leads to the most important features at large frustration. At $\alpha=0.5$ the spectral weight of S_2 is also sizable. Besides the contribution of the two-triplon continuum [inset of Fig. 19(c)] an additional peak appearing for decreasing dimerization can be discerned.

The optical absorption for $R_{\mathrm{NNN}}^{S=0}$ is plotted in Fig. 20. In the insets an enlargement of the line shapes is depicted in order to highlight fine structures. The main difference to the discussion of the optical absorption produced by $R_{\mathrm{NN,weak}}$ are the consequences of the different symmetries of the observables. R_{NNN} suppresses the spectral weight for large momenta. Thus the optical response is weak due to the phonon form factor which stresses large momenta. In addition, the van-Hove singularity resulting from $k=\pi$ of S_1 is suppressed so that only a weak shoulder can be observed at low energies, independent of frustration and dimerization. At $\alpha=0.25$ the additional side structures are produced by the bound states S_2 and S_3.

VI. SUMMARY

In this work we have presented results for the spectral densities of the dimerized and frustrated Heisenberg chain. We used a perturbative realization of the continuous unitary transformations starting from the limit of isolated dimers. By the transformations an effective model is obtained which conserves the number of triplons. Results for the one-triplon and the two-triplon contribution to the spectral density have been shown for strong ($\lambda=0.3$) and intermediate ($\lambda=0.6$) dimerization and for various values of the frustration ($\alpha=0;0.25;0.5$) and for total spin one and zero.

In the first part of this paper we examined the dynamical structure factor which is relevant for inelastic neutron scattering experiments. The one-triplon contribution contains most of the spectral weight at strong and intermediate dimerization. We provided results for the one-triplon dispersion $\omega(k)$ and the k-resolved spectral weight $I_1(k)$. The one-triplon dispersion becomes larger on lowering the dimerization while it becomes flatter on increasing the frustration. The spectral weight $I_1(k)$ is mainly concentrated at $k=\pi$. In the limit $\lambda\to 1$ the one-triplon contribution vanishes except for $\alpha=0.5$ around $k=\pi/2$.

Subsequently we discussed the two-triplon contribution to the dynamical structure factor. We have provided results for the spectral density of the two-triplon continuum and for the dispersion and the spectral weight of the two-triplon bound states.

For the unfrustrated spin chain, the spectral weight is concentrated at the lower band edge at larger momenta. Two-triplon bound states only exist in a finite region about $k=\pi/2$. Increasing the frustration leads to a shift of spectral weight to higher energies. At $\lambda=0.6$ and $\alpha=0.5$, the spectral weight is shifted almost totally to the upper band edge at $k=\pi$. This transfer of spectral weight is also found for $\lambda=1$ by exact diagonalization at finite temperatures.[51]

The behavior of the lower band edge changes strongly on varying the frustration. Generically, we find a square-root behavior of the lower band edge. It is a consequence of the hardcore interaction between the triplons which makes it difficult for them to pass each other. In contrast to this result, we find a square-root divergence at the lower band edge for $\alpha=0.25$. Here the energy of a two-triplon bound state is degenerate (to the precision of our analysis of about 2% of J) with the lower band edge of the two-triplon continuum.

We compared the latter finding with results obtained from field theory.[34] In contrast to our finding for the unfrustrated spin chain, field theory predicts a square-root divergence for the lower band edge of the dynamical structure factor of the sine-Gordon model. Thus the commonly used reduction of the spin chain to a sine-Gordon by neglecting the marginal operator cannot be justified quantitatively, at least not for the values of dimerization considered here. We showed that in

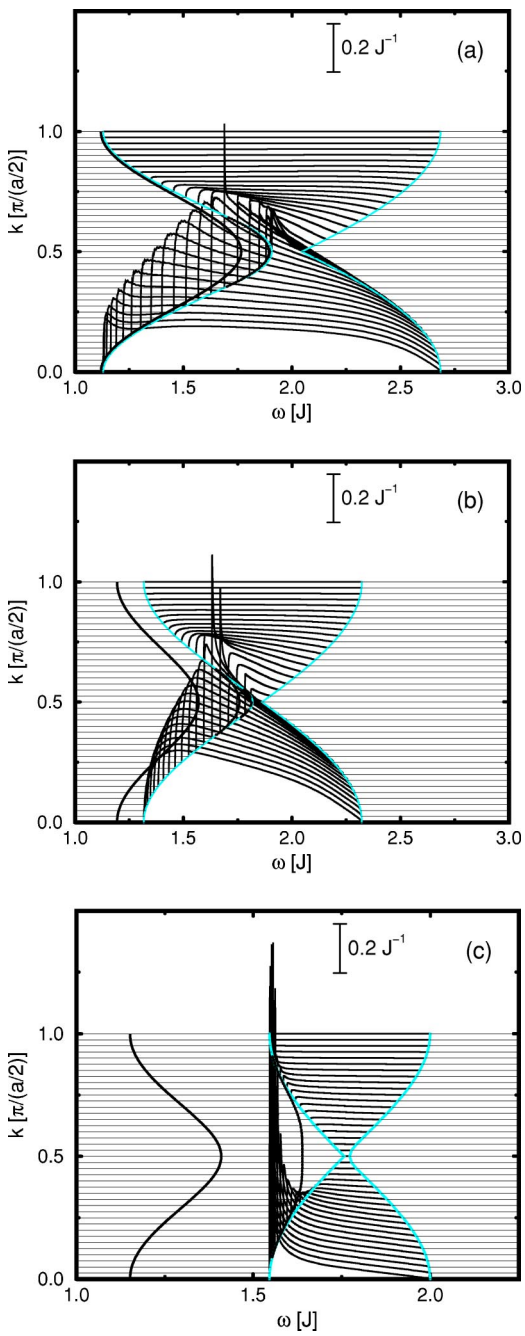

FIG. 16. Two-triplon spectral density $I_2(k,\omega)$ for $R^{S=0}_{\mathrm{NNN}}$ with $\lambda=0.6$ and $\alpha=0.0$ (a), $\alpha=0.25$ (b), and $\alpha=0.5$ (c). Gray lines denote lower and upper bound of the continuum. Black lines indicate dispersion of two-triplon bound states.

the self-consistent harmonic approximation (corresponding to renormalization in first order) the marginal operator $D\cos(4\Phi)$ is as important as the mass operator $\delta\cos(2\Phi)$ at any finite dimerization. Renormalization in second order, however, predicts a slow logarithmic suppression of the marginal term[64] below critical frustration.

We find that square-root behavior represents the generic behavior. A square-root divergence occurs if a two-triplon bound state is degenerate with the lower band edge of the continuum. In the field theoretic language this degenerate bound state, which has not yet emerged from the continuum, is the third breather. We find the concomitant square-root divergence for $\alpha\approx\alpha_{0,c}$.

The applicability of the sine-Gordon model to the unfrustrated, but finitely dimerized spin chain is further questioned by the study of the excitation energies of the bound states. The ratio of the excitation energies of the $S=0$ two-triplon bound state and the one-triplon gap is exactly $\sqrt{3}$ in the SU(2)-symmetric sine-Gordon model. We find this ratio only for $\alpha_0=\alpha_{0,c}$ in agreement with a previous numerical study.[37] At present, we do not know why $\alpha_0=\alpha_{0,c}$ is required to retrieve the field-theory result for the second breather, but $\alpha\approx\alpha_{0,c}$ to retrieve the field theory result for the third breather. It is to be expected that one has to go to very much lower values of the dimerization, i.e., closer to $\lambda=1$, to retrieve the behavior of a pure sine-Gordon model. But as long as the dimerization is *not* extremely small the marginal operator cannot be neglected for a quantitative description. Thus, the effective low-energy model to be considered is the double sine-Gordon model for which the SU(2) symmetry condition will be different from $K=1/2$ and hence also the ratios of the breather energies will differ from the ratios known for the sine-Gordon model.[60]

In the second part of this work, we discussed spectral properties of the dimerized and frustrated spin chain for excitations with total spin zero which are relevant for optical experiments. We presented results for the two-triplon contribution which contains most of the spectral weight.

We examined two different observables: a NN coupling on the weak bonds $R^{S=0}_{\mathrm{NN,weak}}$ and a NNN coupling $R^{S=0}_{\mathrm{NNN}}$. The observables obey different symmetries. The NN coupling possesses a reflection symmetry about $k=\pi/2$. The NNN coupling does not have any reflection symmetry except for $k=\pi$ where it is odd so that no even $S=0$ two-triplon state can be excited. The spectral densities for both observables are dominated by the two-triplon bound state S_1 which contains most of the spectral weight. This bound state exists for all momenta, independent of dimerization and frustration. The binding energy increases by turning on the frustration.

The spectral weight of the two-triplon continuum is concentrated at the lower band edge for all considered values of dimerization and frustration. For finite dimerization, the lower band edge displays a square-root behavior for $\alpha=0.25$ in accordance with the results of the sine-Gordon model. Divergences may occur only at exactly zero dimerization. The behavior changes similarly to the $S=1$ case if a two-triplon bound state is almost degenerate with the lower band edge of the two-triplon continuum. Such a degeneracy appeared in our data for $\alpha\approx0$ and for $\alpha\approx0.5$.

Finally, we presented results for the Raman response and the infrared absorption. Both experiments are dominated by the bound state S_1 for the values of dimerization considered here. This bound state produces two van-Hove singularities in the infrared absorption resulting from $k=\pi/2$ and $k=\pi$. The van-Hove singularity at lower energies becomes more important for larger values of the frustration.

VII. CONCLUSIONS

We have shown that continuous unitary transformations (CUT's) are an excellent tool to calculate spectral densities

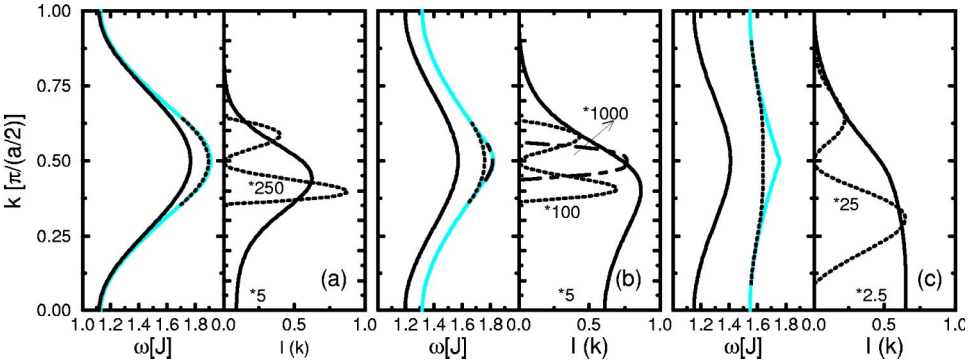

FIG. 17. Two-triplon bound states for $R^{S=0}_{\mathrm{NNN}}$ with $\lambda=0.6$ and $\alpha=0.0$ (a), $\alpha=0.25$ (b) and, $\alpha=0.5$ (c). Left panels show the dispersion of the bound states; right panels show the spectral weights of the bound states multiplied by the indicated factors. Gray lines denote lower bound of the continuum.

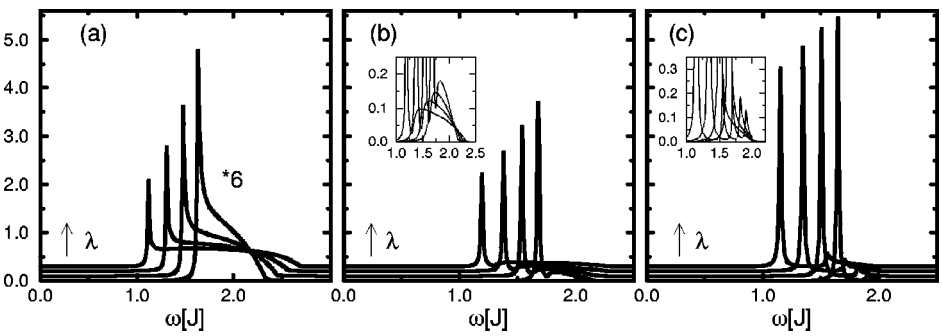

FIG. 18. Raman line shape for $R^{S=0}_{\mathrm{NNN}}$ with additional broadening $\Gamma=0.01$: (a) $\alpha=0$ (b) $\alpha=0.25$ (c) $\alpha=0.5$. In each picture, curves for $\lambda=\{0.3;0.4;0.5;0.6\}$ are shown, shifted for increasing λ in y direction. The Raman response for $\alpha=0$ is multiplied by 6. The insets in (b) and (c) zoom on the continua.

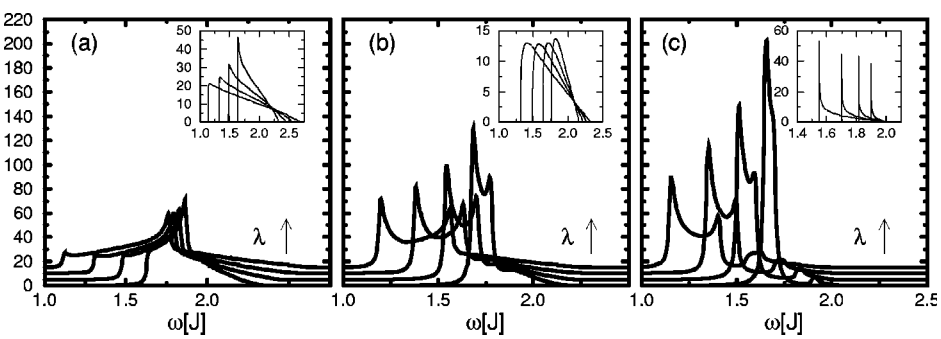

FIG. 19. Optical absorption for $R^{S=0}_{\mathrm{NN,weak}}$ with additional broadening $\Gamma=0.01$: (a) $\alpha=0.0$ (b) $\alpha=0.25$ (c) $\alpha=0.5$. In each picture, curves for $\lambda=\{0.3;0.4;0.5;0.6\}$ are shown. Insets: Contribution of the two-triplon continuum without broadening.

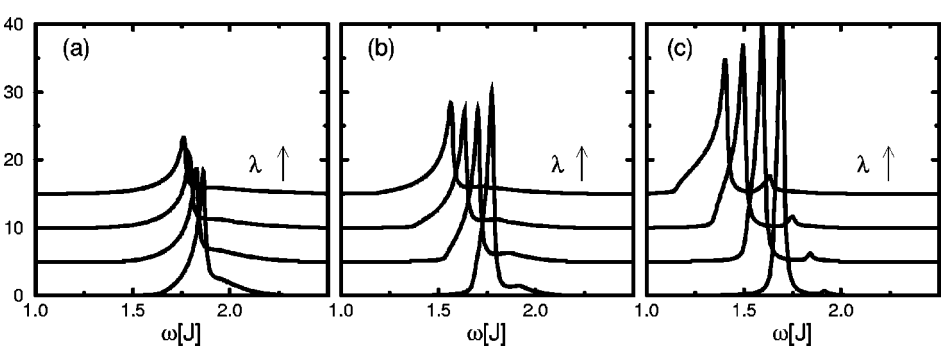

FIG. 20. Optical absorption for $R^{S=0}_{\mathrm{NNN}}$ with additional broadening $\Gamma=0.01$: (a) $\alpha=0.0$ (b) $\alpha=0.25$ (c) $\alpha=0.5$. In each picture, curves for $\lambda=\{0.3;0.4;0.5;0.6\}$ are shown.

in high resolution for the dimerized and frustrated Heisenberg chain. We provided a detailed study of the spectral densities and extracted the generic features of the spectral properties. These data will help to analyze a large variety of spectroscopic measurements for dimerized and frustrated spin chains systems.

We used a description in terms of triplons (elementary triplets) carrying $S=1$. Previously,[22] we had shown for unfrustrated chains that a description in terms of two triplons is sufficient even in the limit of zero dimerization. The triplon may also serve as an elementary excitation of the uniform Heisenberg chain besides the well-established spinon excitation. In the present work, we found further strong support for this result. The two-triplon spectral densities computed at finite dimerization displayed well-developed precursors of the results for the uniform chain based on spinons, e.g., the dynamical structure factor probing the $S=1$ sector[4] or the optical absorption[74] probing the $S=0$ sector.

In the frustrated case it is yet an open issue whether a triplon description works also in the limit of zero dimerization. Especially the gapped phase ($\alpha_0 > \alpha_{0,c}$) requires that the two-spinon continuum between Δ and 2Δ can be described by a dense distribution of bound many-triplon states. For this to occur an infinite-range effective interaction is necessary which is beyond the scope of the perturbative CUT's. But we take the nice agreement between the shifts of spectral weight obtained by complete exact diagonalization at finite temperatures[51] for the undimerized frustrated chain with our results at finite dimerization as indication that the triplon description can be extended to the undimerized frustrated chain, too.

The comparison of our results to those obtained by mapping the spin chain to a sine-Gordon model led to a number of insights. Both approaches agree that the generic singularity at the lower band edge is a square-root, either a divergence or a zero. The divergence occurs if and only if a bound state is degenerate with the band edge. It turned out that the predictions of the single sine-Gordon model hold for critical frustration only which agrees with previous conclusions based on numerical results.[37] The general spin chain at nonvanishing dimerization requires to go beyond the single sine-Gordon model. We showed analytically that in the self-consistent harmonic approximation (equivalent to first order renormalization) the Umklapp term is as large as the mass term.[65]

The present study based on perturbative continuous unitary transformation is limited by the tractable maximum range of hopping and interaction processes which correlates with the maximum order. Thus an investigation of the spectral properties for small and zero gaps, i.e., dimerizations, will require to develop new methods allowing for larger ranges (correlation lengths). The continuous unitary transformations do not need to be realized perturbatively. Ongoing research[68] deals with a self-similar realization which renders the treatment of larger ranges possible. In this way, a closer look at critical systems and systems with massive spinons will come within reach.

ACKNOWLEDGMENTS

We thank A. M. Tsvelik, I. Affleck, G. Japaridze, A. Reischl, A. Gössling, M. Grüninger, and E. Müller-Hartmann for stimulating and encouraging discussions and the DFG for financial support under the Grant Nos. SP 1073 and SFB 608.

[1] F.D.M. Haldane, Phys. Rev. B **25**, 4925 (1982).
[2] J. des Cloizeaux and J.J. Pearson, Phys. Rev. **128**, 2131 (1962).
[3] L.D. Faddeev and L.A. Takhtajan, Phys. Lett. **85A**, 375 (1981).
[4] M. Karbach, G. Müller, A.H. Bougourzi, A. Fledderjohann, and K. Mütter, Phys. Rev. B **55**, 12 510 (1997).
[5] C. Knetter, K.P. Schmidt, M. Grüninger, and G.S. Uhrig, Phys. Rev. Lett. **87**, 167204 (2001).
[6] K.P. Schmidt, C. Knetter, and G.S. Uhrig, Europhys. Lett. **56**, 877 (2001).
[7] W. Zheng, C.J. Hamer, and R.R.P. Singh, Phys. Rev. Lett. **91**, 037206 (2003).
[8] C.J. Hamer, W. Zheng, and R.R.P. Singh, Phys. Rev. B **68**, 214408 (2003).
[9] M. Hase, I. Terasaki, and K. Uchinokura, Phys. Rev. Lett. **70**, 3651 (1993).
[10] M. Nishi, O. Fujita, and J. Akimitsu, Phys. Rev. B **50**, 6508 (1994).
[11] J. Riera and A. Dobry, Phys. Rev. B **51**, 16 098 (1995).
[12] G. Castilla, S. Chakravarty, and V.J. Emery, Phys. Rev. Lett. **75**, 1823 (1995).
[13] M. Isobe and Y. Ueda, J. Phys. Soc. Jpn. **65**, 1178 (1996).
[14] A.W. Garrett, S.E. Nagler, D.A. Tennant, B.C. Sales, and T. Barnes, Phys. Rev. Lett. **79**, 745 (1997).
[15] G. Chaboussant, P.A. Crowell, L.P. Lévy, O. Piovesana, A. Madouri and D. Mailly, Phys. Rev. B **55**, 3046 (1997).
[16] G. Xu, C. Broholm, D.H. Reich, and M.A. Adams, Phys. Rev. Lett. **84**, 4465 (2000).
[17] D.A. Tennant, C. Broholm, D.H. Reich, S.E. Nagler, G.E. Granroth, T. Barnes, K. Damle, G. Xu, Y. Chen and B.C. Sales, Phys. Rev. B **67**, 054414 (2003).
[18] S.E. Nagler, D.A. Tennant, R.A. Cowley, T.G. Perring, and S.K. Satija, Phys. Rev. B **44**, 12 361 (1991).
[19] T. Ami, M.K. Crawford, R.L. Harlow, Z.R. Wang, D.C. Johnston, Q. Huang, and R.W. Erwin, Phys. Rev. B **51**, 5994 (1995).
[20] N. Motoyama, H. Eisaki, and S. Uchida, Phys. Rev. Lett. **76**, 3212 (1996).
[21] Previously, we used the term "elementary triplets" to distinguish threefold degenerate elementary excitations from magnons which are the elementary excitations of long-range *ordered* magnets. We henceforth use the term "triplon" instead to have a shorter expression distinguishing more clearly from composite triplets.
[22] K.P. Schmidt and G.S. Uhrig, Phys. Rev. Lett. **90**, 227204 (2003).
[23] R. Jullien and F.D.M. Haldane, Bull. Am. Phys. Soc. **28**, 344 (1983).
[24] K. Okamoto and K. Nomura, Phys. Lett. A **169**, 433 (1992).

[25] S. Eggert, Phys. Rev. B **54**, R9612 (1996).
[26] C.K. Majumdar and D.K. Ghosh, J. Math. Phys. **10**, 1388 (1969).
[27] C.K. Majumdar and D.K. Ghosh, J. Math. Phys. **10**, 1399 (1969).
[28] P.M. van den Broek, Phys. Lett. **77A**, 261 (1980).
[29] B.S. Shastry and B. Sutherland, Phys. Rev. Lett. **47**, 964 (1981).
[30] R. Chitra, S. Pati, H.R. Krishnamurthy, D. Sen, and S. Ramasesha, Phys. Rev. B **52**, 6581 (1995).
[31] A. Luther and I. Peschel, Phys. Rev. B **12**, 3908 (1975).
[32] F.D.M. Haldane, Phys. Rev. Lett. **45**, 1358 (1980).
[33] G.S. Uhrig and H.J. Schulz, Phys. Rev. B **54**, R9624 (1996).
[34] A.O. Gogolin, A.A. Nersesyan, and A.M. Tsvelik, *Bosonization and Strongly Correlated Systems* (Cambridge University Press, Cambridge, UK, 1998).
[35] I. Affleck, in *Dynamical Properties of Unconventional Magnetic Systems*, Vol. 349 of *NATO Advanced Studies Institute, Series E: Applied Sciences*, edited by A.T. Skjeltorp and D. Sherrington (Kluwer Academic, Dordrecht, 1998).
[36] A. Fledderjohann and C. Gros, Europhys. Lett. **37**, 189 (1997).
[37] G. Bouzerar, A.P. Kampf, and G.I. Japaridze, Phys. Rev. B **58**, 3117 (1998).
[38] P. Shevchenko, V.N. Kotov, and O.P. Sushkov, Phys. Rev. B **60**, 3305 (1999).
[39] T. Barnes, J. Riera and D.A. Tennant, Phys. Rev. B **59**, 11 384 (1999).
[40] S. Trebst, H. Monien, C.J. Hamer, Z. Weihong, and R.R.P. Singh, Phys. Rev. Lett. **85**, 4373 (2000).
[41] W. Zheng, C.J. Hamer, R.R.P. Singh, S. Trebst, and H. Monien, Phys. Rev. B **63**, 144410 (2001).
[42] F.J. Wegner, Ann. Phys. (N.Y.) **3**, 77 (1994).
[43] C. Knetter and G.S. Uhrig, Eur. Phys. J. B **13**, 209 (2000).
[44] www.thp.uni-koeln.de/~gu
[45] C. Knetter, K.P. Schmidt, and G.S. Uhrig, Eur. Phys. J. B **36**, 525 (2004).
[46] C. Knetter, K.P. Schmidt, and G.S. Uhrig, J. Phys.: Condens. Matter **36**, 7889 (2003).
[47] K.P. Schmidt, C. Knetter, and G.S. Uhrig, Acta Phys. Pol. **34**, 1481 (2003).
[48] K.P. Schmidt, H. Monien, and G.S. Uhrig, Phys. Rev. B **67**, 184413 (2003).
[49] Even the one-triplon contribution does not vanish completely since there are regions in momentum space where the one-triplon state is stable even at zero dimerization (see also discussion at the end of Sec. IV A).
[50] M. Müller, H.-J. Mikeska, and N. Cavadini, J. Phys.: Condens. Matter **15**, 8513 (2003).
[51] K. Fabricius and U. Löw, Phys. Rev. B **57**, 13 371 (1998).
[52] W.J. Caspers and W. Magnus, Phys. Lett. **88A**, 103 (1982).
[53] W.J. Caspers, K.M. Emmett, and W. Magnus, J. Phys. A **17**, 2687 (1984).
[54] R.R.P. Singh and Z. Weihong, Phys. Rev. B **59**, 9911 (1999).
[55] F. A. Smirnov, *Form Factors in Completely Integrable Models of Quantum Field Theory* (World Scientific, Singapore, 1992).
[56] I. Affleck, Nucl. Phys. **B265**, 409 (1986).
[57] I. Affleck and F.D.M. Haldane, Phys. Rev. B **36**, 5291 (1987).
[58] S.R. White and I. Affleck, Phys. Rev. B **54**, 9862 (1996).
[59] R. Chitra and T. Giamarchi, Phys. Rev. B **55**, 5816 (1997).
[60] R.F. Dashen, B. Hasslacher, and A. Neveu, Phys. Rev. D **12**, 2443 (1975).
[61] T. Nakano and H. Fukuyama, J. Phys. Soc. Jpn. **49**, 1679 (1980).
[62] T. Nakano and H. Fukuyama, J. Phys. Soc. Jpn. **50**, 2489 (1981).
[63] M.C. Cross and D.S. Fisher, Phys. Rev. B **19**, 402 (1979).
[64] I. Affleck, D. Gepner, H.J. Schulz, and T. Ziman, J. Phys. A **22**, 511 (1989); **23**, 4725 (1990).
[65] G.S. Uhrig, Habilitation 1999, www.thp.Uni-Koeln.DE/~gu/veroeffentlichungen.html
[66] E. Müller-Hartman and G.S. Uhrig (unpublished).
[67] W. Zheng, C.J. Hamer, R.R.P. Singh, S. Trebst, and H. Monien, Phys. Rev. B **63**, 144411 (2001).
[68] A. Reischl, E. Müller-Hartmann, and G.S. Uhrig, cond-mat/0401028 (unpublished).
[69] J. Lorenzana and G.A. Sawatzky, Phys. Rev. Lett. **74**, 1867 (1995).
[70] J. Lorenzana and G.A. Sawatzky, Phys. Rev. B **52**, 9576 (1995).
[71] P.A. Fleury and R. Loudon, Phys. Rev. **166**, 514 (1968).
[72] B.S. Shastry and B.I. Shraiman, Phys. Rev. Lett. **65**, 1068 (1990).
[73] M. Windt, M. Grüninger, T. Nunner, C. Knetter, K.P. Schmidt, G.S. Uhrig, T. Kopp, A. Freimuth, U. Ammerahl, B. Büchner, and A. Revcolevschi, Phys. Rev. Lett. **87**, 127002 (2001)
[74] J. Lorenzana and R. Eder, Phys. Rev. B **55**, R3358 (1997).
[75] H. Suzuura *et al.*, Phys. Rev. Lett. **76**, 2579 (1996).